ACTA RADIOLOGICA
EDITA IUSSU SOCIETATUM RADIOLOGICARUM
DANIAE, FENNIAE, NORVEGIAE ET SUECIAE

VOL. 54 AUGUST 1960 FASC. 2

ELECTROKYMOGRAPHIC CHANGES IN MYOCARDIAL INFARCTION

by

OSBORNE BARTLEY

The diagnosis of myocardial infarction is usually based on the clinical signs and electrocardiographic examination. Infarcts may, however, develop without appreciable clinical signs; moreover, an electrocardiographic diagnosis may sometimes be difficult, especially in bundle branch block and when limb leads alone are used. Electrokymography is employed mostly for the diagnosis of valvular diseases of the heart, though also in other lesions, as for instance myocardial infarction. Since the latter condition may be associated with hemodynamic changes, partly of the type observed in certain valvular diseases, it is important to be cognizant of the electrokymographic picture of localized myocardial lesion.

Electrokymographic investigations of the ventricular movements have been reported notably by LUISADA & FLEISCHNER (1948), GILLICK & REYNOLDS (1949), SCHWEDEL, SAMET & MEDNICK (1950), DACK (1950 and 1955), DACK, PALEY & SUSSMAN (1950), and DACK & PALEY (1952). In 1955 the present author described atrial changes in myocardial infarction.

This report will be concerned with the electrokymographic changes observed in the movements of the ventricles, atria and great vessels in a series of verified myocardial infarctions.

From Roentgen Department I (Director: Prof. S. R. Kjellberg) and Roentgen Department II (Director: Docent I. Wickbom), Sahlgrenska Sjukhuset, Gothenburg, Sweden. Submitted for publication 3 February 1960.

Table

Electrokymographic changes in thirty-six cases of myocardial infarction
(The numbers within parentheses indicate cases that could not be evaluated)

	Ventricles				Atria			Great vessel	
	Aneurysm	Distinct	Uncertain	None	Left	Right	Asynchronism	Pulmonary artery	Ascending aort
7 cases (autopsy)....	1	4	2	0	7	5	4	5	3(3
29 cases (no autopsy)	6	15	6	2	21(1)	14(2)	12(2)	9(1)	10(9
Total 36 cases	7	19	8	2	28(1)	19(2)	16(2)	14(1)	13(12
Changes in %.....	72		28		80	56	47	40	54

Methods and Material

The examinations were performed with the aid of a direct-recording electrokymograph (Mingograf 22, Elema), linked with a heart-tone attachment. Electrocardiograms were used as reference curves in all cases and, in the majority, phonocardiography was also carried out simultaneously. All examinations were performed with the patient sitting.

The series consists of 36 patients: 29 males aged from 28 to 73, and seven females aged from 55 to 72. In 35 cases the diagnosis of myocardial infarction was based on the clinical picture and electrocardiograms. In some of them the electrocardiographic findings at the electrokymographic examination were ambiguous, but verification was subsequently obtained on further examination with special leads. One patient, a 31-year-old man, had obvious infarction changes at electrokymographic examination, but neither the clinical findings nor electrocardiography with limb leads alone lent support to the diagnosis. At autopsy 10 days after the electrokymographic examination a typical infarct was found at the site indicated in the electrokymogram. In 7 of the 36 cases the diagnosis was verified as above and also at autopsy.

The examinations were performed at varying times after the onset of symptoms: from less than three weeks to several years.

The results are tabulated in the Table above.

Movements of the ventricles. These movements have been described in detail, notably by Dack. According to him, abnormal ventricular movements may occur either during systole or diastole, or during both. The changes during systole consist of either a localized reduction or absence of movement during

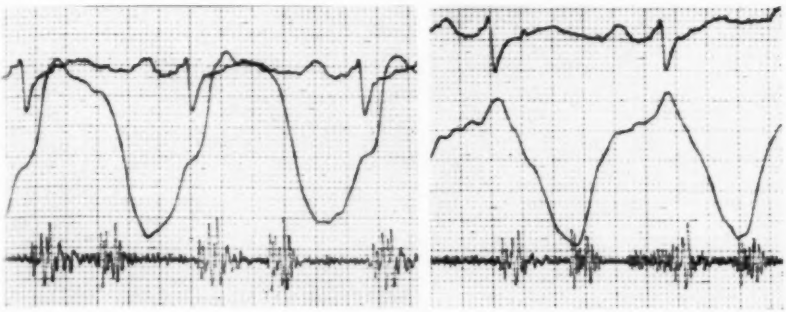

Fig. 1. Cardiac aneurysm. a) Record from the aneurysm: completely paradoxical curve during systole and early diastole; same appearance, in principle, as a pressure curve from the ventricle. b) Above the aneurysm: no appreciable abnormality; the curve has largely the same appearance as the volume curve from a normal ventricle.

the ejection phase, or a partially or completely paradoxical movement. For a movement to be classed as partially paradoxical the ventricle must move laterally during the maximum ejection phase for a period exceeding 0.08 sec. In completely paradoxical movement the ventricle moves laterally instead of medially during systole, and medially instead of laterally at the onset of diastole. The curve then has the appearance of a pressure curve from the ventricle rather than a volume curve, as in normal conditions. The abnormalities during diastole consist of either retardation or absence of the lateral movement, or a medial movement in early diastole, or a completely paradoxical movement.

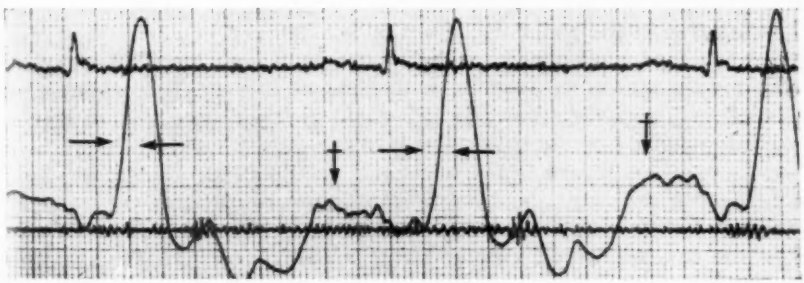

Fig. 2. Partially paradoxical curve. The ventricle moves laterally for 0.10 sec (between the arrows ←). In addition: retarded lateral movement of the ventricle during diastole and abnormal medial movement during the latter part of diastole (↔).

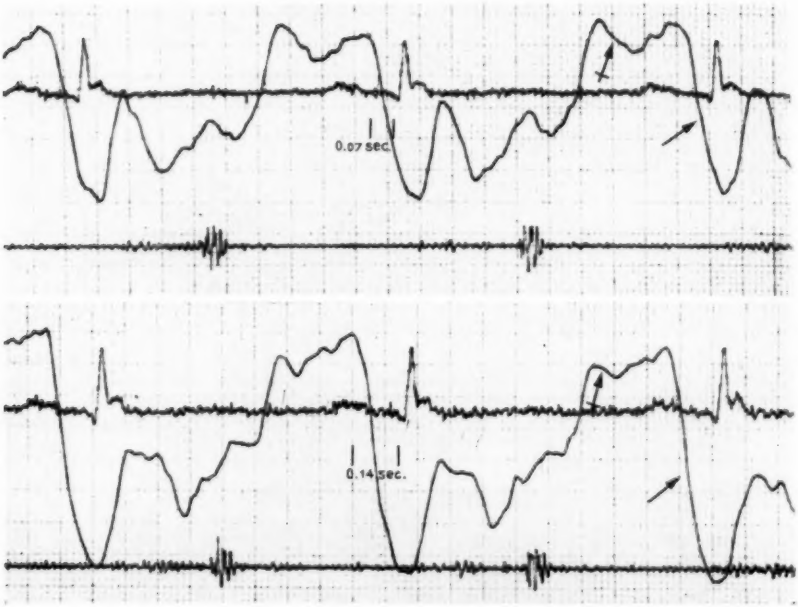

Fig. 3. Atrial curves from a case with cardiac aneurysm: upper, from the left, and lower from the right atrium. Considerably amplified atrial contraction (←) on both sides, pointing to obstructed flow from the atria. The amplitude of the atrial contraction is substantially greater than that of the rapid filling phase (↔). There is atrial asynchronism of approximately 0.07 sec; the right atrium contracts before the left.

The completely paradoxical ventricular movement during systole is, hemodynamically, a sign of cardiac aneurysm. This change was observed in seven of the 36 cases in this series (Fig. 1). 'Distinct changes' in this context implies a partially paradoxical movement during systole, either alone or in conjunction with other changes in the ventricular movements (Fig. 2). Such changes were observed in 19 of the cases. By 'uncertain changes' is meant an observed localized reduction, or absence of movement during systole, as well as the diastolic movements which DACK classed as abnormal. Uncertain changes were found in eight cases, and no ventricular changes whatsoever were noted in two.

Definite changes, in the form of either aneurysm or partially paradoxical movements, were accordingly detected in 26 cases, i. e. 72 per cent. Uncertain changes or none at all in the ventricular movements were recorded in 10 cases or 28 per cent.

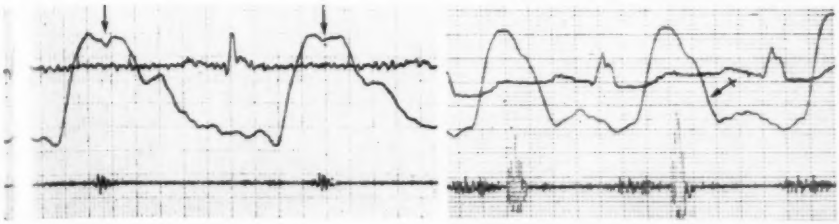

a b

Fig. 4. Curves from the pulmonary artery. a) Changes suggestive of elevated pressure in the pulmonary circulation, with late and somewhat slow upstroke, and high, almost obliterated incisura (←). b) Early diastolic collapse (↔) of the vessel; somewhat late and slow upstroke and fairly high incisura, possibly indicative of a slightly elevated pressure in the pulmonary circulation.

Movements of the atria. In healthy subjects examined in the sitting position most of the blood runs from the atria to the ventricles during the rapid filling phase, when there is a pressure gradient between auricles and ventricles and only a minor part during the active contraction phase of the auricles. In 1955 the present author showed that changes suggestive of an obstructed flow from the left auricle were fairly common in patients with cardiac infarction. The abnormality consisted of a greatly amplified active contraction of the auricle. The auricular changes were thus, on the whole, of the type described notably by ANDERSSON (1953) in mitral disease. By 'pathologic auricular contraction' is in this paper meant a contraction, the amplitude of which exceeds that of the rapid filling phase (Fig. 3). The contraction of the left auricle was evaluated in 35 of the 36 cases; one patient had auricular fibrillation. Pathologic contraction was noted in 28 cases, i. e. 80 per cent. The contraction of the right auricle could be evaluated in 34 cases, being abnormal in 19 cases, or 56 per cent.

LUISADA & FLEISCHNER (1947) among others, have shown electrokymographically that in normal cases the right auricular contraction may precede the left by up to 0.03 sec. In accordance with the observations of previous authors, abnormal asynchronism in the auricular contractions was thus considered to be present when it amounted to more than 0.03 sec. Such asynchronism was found in 16 of 34 cases, or approximately 47 per cent. The greatest asynchronism observed amounted to 0.07 sec and occurred in two patients with cardiac aneurysm (Fig. 3). Right auricular contraction preceded the left in all cases.

Abnormal movements of the pulmonary artery and ascending aorta. The electrokymographic curve from the pulmonary artery and ascending aorta has in normal cases largely the same appearance as the pressure curve from those

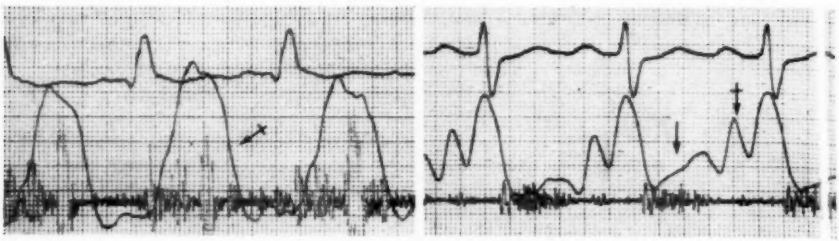

a b

Fig. 5. a) Curve from the ascending aorta. Early diastolic collapse (↔) of the vessel. No distinct incisura. b) case of aortic stenosis, but no extensive localized myocardial lesions at autopsy; this notwithstanding, partially paradoxical ventricular movement in systole (←) as well as abnormal diastolic movements (↔).

vessels. The semilunar valves close at the incisura, and immediately following it there is a small dicrotic wave. The curve then falls to its minimum, which is reached at the next systole.

Evaluable pulmonary artery curves were obtained in all save one of the present cases. Changes, which were of two different types, were observed in 14 cases. In eight of these (Fig. 4a) they consisted of abnormal movements with a late and slow upstroke and a high, often obliterated incisura. Such changes are, according to RUDHE (1956), indicative of pulmonary hypertension. The other type of abnormal movement was found in six cases and took the form of a conspicuously rapid collapse of the vessel immediately following the dicrotic wave. The curve had thus already reached its minimum in early diastole (Fig. 4b).

Evaluable curves were obtained from the ascending aorta in 24 of the 36 cases; the remainder had known or suspected aortic valvular disease and were therefore discarded. Thirteen of the 24 showed, as in the pulmonary artery, a strikingly rapid collapse of the vessel (Fig. 5a).

Discussion

The explanation of the completely paradoxical ventricular curve during systole may well be that the muscular wall is so severely damaged that it cannot withstand the intraventricular pressure during systole. Movements of the wall will then be dependent on the changes of pressure in the ventricle. The completely paradoxical movement of the ventricle does not, however, demonstrate the presence of a cardiac aneurysm. Thus SCHWEDEL et coll. observed paradoxical movements during systole in three patients who, at autopsy, had no demonstrable infarctions; GILLICK & REYNOLDS made simila-

observations. DACK et coll. reported having noted paradoxical ventricular pulsations in e. g. some cases of aortic insufficiency, but never in normal cases. They had also found a false paradoxical movement in normal subjects who had performed Valsalva's maneuver, an observation which I have been able to confirm. In order to reduce the possibility of overdiagnosis of cardiac aneurysm it is therefore advisable, in my opinion, to see that the patient, on examination, holds his breath midway and does not perform a Valsalva maneuver. Furthermore, the paradoxical movement should be detectable only in a circumscribed part of the ventricle, and normal or minor pathologic ventricular movements should be observed contiguous to the presumptive cardiac aneurysm.

The fact that the less-marked paradoxical movement is observed during the initial part of the maximum ejection phase suggests that the wall is partially infarcted and therefore unable to withstand the rapid rise of pressure during that phase. It is the commonest abnormal ventricular movement associated with myocardial lesions, but is not pathognomonic of localized disease for I have observed it in a 40-year-old man with stenosis of the aorta. This patient died two days after the examination. Autopsy disclosed numerous small discrete scars in the myocardium and marked hypertrophy and dilatation of the left ventricle in particular, but no localized myocardial damage that might have been suspected at electrokymography (Fig. 5b).

A reduction or absence of movement of the ventricular wall in a certain segment may attend pathologic processes outside the myocardium, for instance pericarditis and pleural lesions; this should therefore not be judged to be of definite pathologic significance unless there are concomitant changes pointing to myocardial infarction. The changes during diastole are more difficult to explain and probably are not pathognomonic of myocardial infarction. This applies in particular to the retarded or absent filling during the rapid filling phase which I have observed in both aortic valvular disease and hypertension without infarction.

The changes in atrial movements associated with myocardial infarction are, as pointed out above, suggestive of an obstructed flow from the atria. They are not pathognomonic of myocardial infarction but are found in e. g. organic mitral valve disease (ANDERSSON 1953), aortic valvular lesions and hypertension (BARTLEY 1955), and constrictive pericarditis (RUDHE 1956). The most plausible explanation of the impeded flow from the atria in infarction may be that the ventricular pressure in diastole is elevated, due, either to myocardial failure with a residual blood volume, or to impaired distensibility of the ventricle. The active contraction will then have to be increased in order to maintain the stroke volume.

It is not clear why, in myocardial infarction, abnormal asynchronism is frequently observed in the contraction of the atria. The cause may be, for example, an intra-auricular conduction disturbance with dilatation and

hypertrophy of the left auricle, though the possibility of concomitant atrial infarction cannot be ruled out.

The high pressure changes in the pulmonary artery point to left ventricular failure with back pressure. The other type of arterial change that was observed (the early diastolic collapse) is, however, somewhat more difficult to explain. I have seen this change in patients with a low stroke volume, which is probably responsible in most cases for the observed change in arterial pulsations in myocardial infarction. Even this change, however, is not pathognomonic; I have noted it in several cases of e. g. hypertension without a reduced stroke volume.

Conclusions

The possibility of demonstrating myocardial lesions electrokymographically is of value from the differential diagnostic point of view. But since none of the changes in the movements of the ventricles, atria and great vessels are in themselves pathognomonic of localized myocardial damage, it is important to study the movements of all the chambers of the heart and of the great vessels, and then to correlate the observations. This should throw far more light on the hemodynamics than a study of the ventricular movements alone; and in this way the electrokymographic diagnosis of myocardial lesions can possibly be improved. In the present series, atrial changes with pathologic contraction and asynchronism were just as common in the absence as in the presence of typical ventricular changes. Only in one case were there neither ventricular changes nor any other demonstrable changes.

SUMMARY

Thirty-six cases of verified myocardial infarction were examined electrokymographically and the movements of the ventricles, atria and great vessels investigated. The diagnostic significance of the changes observed is discussed. Attention is drawn to the value of an electrokymographic study of the movements of the ventricles, atria and great vessels in elucidating the hemodynamics of myocardial infarction.

ZUSAMMENFASSUNG

Sechs-und-dreissig Fälle von verifiziertem Myokardinfarkt wurden elektrokymographisch untersucht, und die Bewegungen der Ventrikel, Atria und grossen Gefässe studiert. Die diagnostische Signifikanz der beobachteten Veränderungen wird besprochen. Es wird auf den Wert einer elektrokymographischen Studie der Bewegungen der Ventrikel, Atria und grossen Gefässe zur Erläuterung der Hämodynamik des Myokardinfarktes hingewiesen.

RÉSUMÉ

Trente-six cas d'infarctus myocardique vérifié ont été examinés électrokymographiquement et les mouvements des ventricules, des oreillettes et des gros vaisseaux ont été étudiés. L'auteur examine l'intérêt diagnostique des modifications observées. Il attire l'attention sur la valeur d'une étude électrokymographique des mouvements des ventricules, des oreillettes et des gros vaisseaux pour élucider l'hémodynamique de l'infarctus du myocarde.

REFERENCES

ANDERSSON, T.: Electrokymographic examinations in mitral valve disease. Acta radiol (1953) Suppl. No. 106.

BERTLEY, O.: Patologisk förmakskontraktion, registrerad med elektrokymografi. (In Swedish.) Paper read at the Meeting of the Northern Association of Radiology, Gothenburg, June 1955.

DACK, S.: Left ventricular border motion. Proc. 1st conference of Electrokymography 1950, p. 15. U. S. Government Printing Office, Washington 1951.

– The ventricular pulsations in myocardial infarction; a fluoroscopic and kymographic study. Dis. Chest 27 (1955), 282.

– and PALEY, D. H.: Elektrokymography. I. The ventricular electrokymogram. Amer. J. Med. 12 (1952), 331.

– — and SUSSMAN, M. L.: A comparison of electrokymography and roentgenkymography in the study of myocardial infarction. Circulation 1 (1950), 551.

GILLICK, F. G. and REYNOLDS, W. G.: Clinical application of electrokymography. Calif. Med. 70 (1949), 407.

LIMSADA, A. A. and FLEISCHNER, F. G.: Temporal relation between contraction of right and left sides of the normal human heart. Proc. Soc. exp. Biol. 66 (1947), 436.

– — Studies of fluorocardiography: Tracings of the left ventricle in myocardial infarction. Acta cardiol. 3 (1948), 308.

RUDHE, U.: Electrokymography. With special reference to valvular pulmonary and infundibular stenosis. Acta radiol. (1956) Suppl. No. 134.

SCHWEDEL, J. B., SAMET, P. and MEDNICK, H.: Electrokymographic studies of abnormal left ventricular pulsations. Amer. Heart J. 40 (1950), 410.

SUSSMAN, M. L., DACK, S. and PALEY, D. H.: Some clinical applications of electrokymography. The findings in myocardial infarction and heart block. Radiology 53 (1949), 500.

FROM THE ROENTGENDIAGNOSTIC DEPARTMENT (DIRECTOR: U. RUDHE) OF THE PEDIATRIC CLINIC, KAROLINSKA SJUKHUSET, STOCKHOLM, SWEDEN.

FRACTURES AT THE TUBEROSITY OF THE FIFTH METATARSAL BONE IN CHILDREN

by

HERBERT MÜSSBICHLER

The fractures at the base of the fifth metatarsal bone (M5) are generally considered to unite slowly and sometimes remain ununited (BÖHLER, EHALT, PREISS). Only a few notes on this particular type of fracture in children could be found in the literature (BLOUNT, RETTIG, CHIGOT and ESTÈVE, inter al.), a fact which prompted the present investigation.

Anatomy. The lateral part of the base of M5 is formed by the tuberosity which is usually part of the diaphysis. As a rare anomaly the base may be formed as an accessory bone center, separated from the diaphysis by epiphyseal cartilage (Fig. 1f). This pseudo-epiphysis usually appears between the second and fifth years of life. The epiphyseal line should not be mistaken for a fracture.

The growth of the tuberosity on its lateral and plantar aspects takes place in the epiphysis and varies considerably in size, shape and position (Fig. 1, a to e). These variations are mainly due to its stage of ossification and have been well illustrated by ZIMMER. According to ISELIN and SCHOUWEY the epiphysis is invariably present at the age of 15 years.

Only six cases of 'os Vesalianum' were described up to 1922 (BAASTRUP, JOHANSSON). It was said to occur in the angle between the cuboid bone and the tuberosity of M5. LANZ and WACHSMUTH, WENZELGRUBER, and PFITZER never came across this bone in a large series of anatomic dissections and doubted its existence.

Submitted for publication 16 November 1959.

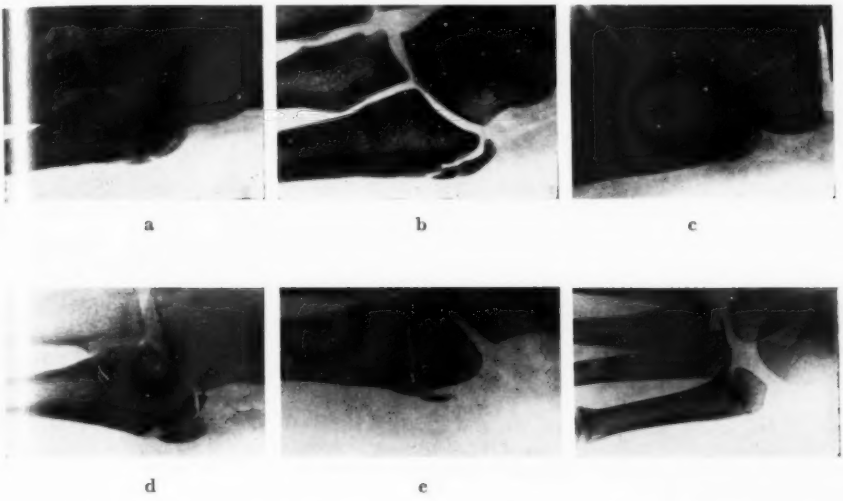

a b c

d e

Fig. 1. a, b, c) Normal anatomy of the tuberosity of M5, in a 12-year-old girl, in a. p., oblique and lateral views. The epiphysis consists of two parts, the border of the epiphyseal line is wavy, and the adjacent soft tissue shows distinct margins. d) and e) Normal tuberosity but swelling of surrounding soft tissue due to trauma. Epiphyses shown in (a) to (e) represent normal variations. Small bone centers (↔) belonging to the epiphysis. f) Accessory bone center in the prox. end of M5 in a 4-year-old girl. The epiphyseal line (→) should not be mistaken for a fracture.

Case material

Of the 1 668 patients who were referred to the surgical unit of the pediatric clinic during the years 1952—1959 for injuries of the feet and ankles, 567 had fractures of the metatarsal bones. Sixty-six of these were situated in the region of the tuberosity of M5. These cases form the basis of the present study. A survey of the material of injuries of the feet and ankles in adults collected at the roentgendiagnostic department, 603 cases in all, of which 244 had fractures of the metatarsal bones and 66 had fractures at the tuberosity of M5, thus showed a higher figure in this age group.

All but one of the fractures occurred in children above the age of $10^1/_2$ years; the exception was a fracture in a child of $7^1/_2$ years of age.

The fractures were distributed equally among boys and girls. They were classified into the following types (Fig. 3):

1. Transverse fractures
2. Oblique and longitudinal fractures (regarded as atypical)
3. Avulsions
4. Epiphyseal separation

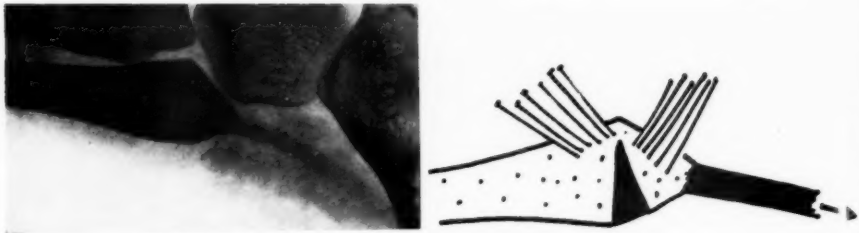

a b

Fig. 2. a) Normal soft tissue showing insertion of tendon of peroneus brevis muscle. b) Sketch of the same region with ligaments, and a transverse fracture added to show the effect of traction of the peroneus brevis muscle upon the fragment. Blackened portions: wedge-shaped diastasis and peroneus brevis muscle. Ligaments connecting M5 with M4 and cuboid bone are indicated by the stripes, and the direction of muscular traction by the arrow.

In all cases a more or less marked swelling of the soft tissue around the tuberosity was present. This feature was often helpful in establishing the correct diagnosis, particularly in cases of avulsions or fissures. In nearly all patients, the fractures were the result of a severe inversion sprain of the foot. Direct violence in the form of a blow or a kick was reported in 6 cases. In one case there was no history of trauma.

Transverse fractures. In 5 out of 53 fractures of this type a diastasis of 2 to 5 mm was present at the first examination carried out on the day of the accident (Fig. 7a); in the remaining cases the separation of the fragments was less. During the process of healing the diastasis between the fragments increased in size in all these cases and took the shape of a wedge-formed defect, the tip of which lay medially (Figs 2b, 4, 5). The diastasis was invariably present in the films obtained 1 to 4 weeks after the accident. Another regular feature was that the callus formation, which usually appeared 3 to 4 weeks after the accident (Fig. 4b), was restricted to the endosteum, as a result of which the fracture surfaces appear sclerotic. No further increase in the diastasis was observed in the period following this stage. The appearance of the diastasis was not related to the type of treatment given.

In the further healing process callus was laid down at the inner side of the wedge-formed defect and appeared last at its lateral aspect (Fig. 4c). The absence of periosteal reaction

Fig. 3. Type and position of 66 fractures at the tuberosity of M5 in children. Full lines indicate transverse fractures (53), interrupted lines atypical fractures (5) and the circles avulsions (8).

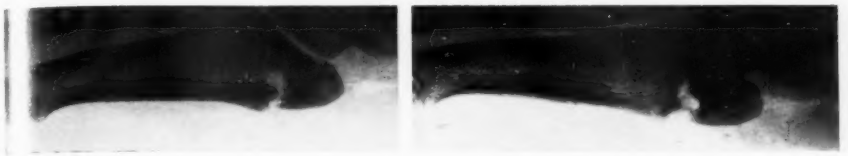

a b

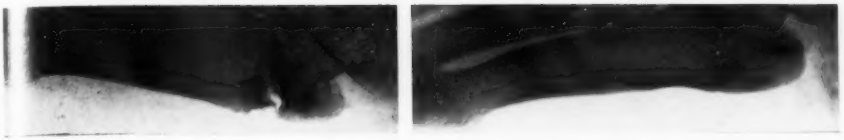

c d

e

Fig. 4. Follow-up study of a transverse fracture in a 14-year-old boy. a) Recent fracture. b) After one month of treatment in plaster, diastasis and sclerosis due to callus. c) Six weeks after (a), increasing amount of callus between the fragments. d) 3 3/4 years after the accident, only slight deformity with elongation of the tuberosity. e) Healthy side for comparison.

is explained by the fact that the fractures involve that part of the bone where no periosteum is present. *Anatomic dissections* performed by the author on two specimens showed that the tuberosity and its adjacent surroundings were wholly occupied by the attachments of the ligaments and the tendon of the peroneus brevis muscle, which is in agreement with the illustrations given in the text-books of anatomy (RAUBER-KOPSCH inter al.).

In some cases the diastasis and the sclerosis due to newly formed bone tissue were so marked as to give the impression of developing non-union (pseudoarthrosis).

Twenty-one of the transverse fractures, selected at random, were re-examined 4 to 9 weeks after the accident with a view to studying the healing process; at that time none of them showed complete union of the fragments. In follow-up examinations, performed 4 months to 4 years after the injury, union had, however, occurred in all cases; in one single case examined at 10 weeks, union had already taken place. No noteworthy deformity of the tuberosity was observed except for slight lengthening (Fig. 4d) as revealed by a comparison with the unaffected side. Plaster had been applied for 1 to 8 weeks in 18 cases and only elastoplast in 3 cases. Most of them were free of symptoms after one or two weeks of treatment.

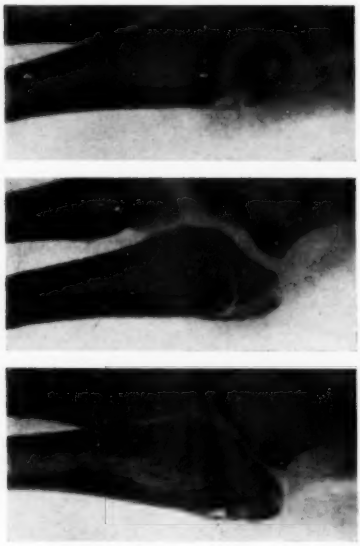

Fig. 5

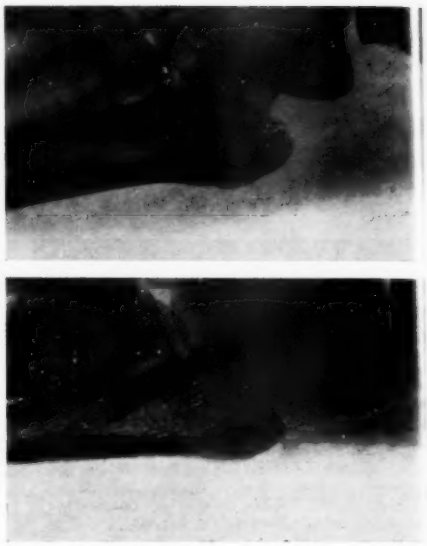

Fig. 6

Fig. 5. Transverse fracture of the tuberosity and epiphysis in a 11-year-old girl. Top view: recent fracture. Middle: three weeks after the former, and after 2 weeks in plaster. Diastasis has increased. Lower view: four months after the injury, the fracture is healed and the epiphysis has united with the tuberosity.

Fig. 6. Recent atypical fractures. Top view: oblique. Lower view: longitudinal fracture with a small superficial fragment. There is a marked soft tissue swelling.

Oblique and longitudinal (atypical) fractures. Two fractures ran parallel to the axis of the diaphysis while 3 cases showed an oblique course of the fracture line across the tuberosity; in one of the cases a small superficial fragment was evident (Fig. 6b). The fractures were consistently discrete. The two longitudinal fractures were re-examined after an interval of 2 and 4 weeks respectively and found to have healed. Complete union was present in 2 oblique fractures studied at 6 months and at $2\,^1/_2$ years respectively. No diastasis or sclerosis occurred in these cases. No follow-up examination was made in the remaining case.

Avulsions. In 8 cases small flakes of bone were noted at the tuberosity (Fig. 6b). Plaster was applied for one to several weeks. The time of complete union was not different from that observed in the transverse fractures. No displacement of the fragments occurred.

a b c

Fig. 7. Epiphyseal separation associated with a transverse fracture. a) Immediately after the injury: epiphysis (←○) and fragment (←). b) Two months later (plaster applied for 1 1/2 weeks): the epiphysis has united with the fragment. c) Healthy side for comparison.

Epiphyseal separation. Only one case showed evidence of separation of the epiphysis. This was combined with a transverse fracture of the tuberosity and marked displacement of the proximal fragment (Fig. 7).

Discussion

In spite of earlier statements (BAASTRUP, inter al.) fractures at the base of M5 are evidently not rare. The reasons for the delayed union of the transverse type of these fractures as well as of the avulsions is in all likelihood due to the effect of traction of the peroneus brevis muscle which is inserted at the tuberosity (Fig. 2). This results in an increase of the diastasis between the fragments. In children this will ultimately not interfere with healing, as complete union can be expected 10 weeks or later after the injury. This series of events does not seem to be influenced to any apparent degree by the type of fixation applied. The use of plaster neither prevents further separation of the fragments (diastasis) nor does it accelerate the healing process. Fixation thus mainly serves the purpose of relieving pain, and should be removed after one or two weeks. The lesions in adults are as a rule more extensive than in young people which may contribute to the deficient healing described by EHALT and PREISS, inter al.

SUMMARY

Sixty-six fractures at the tuberosity of the fifth metatarsal bone out of a total material of 1 668 cases of injuries of the feet and ankles in children were studied according to frequency, type and healing. The transverse fractures and the avulsions were all characterized by a prolonged healing time. Ultimately, however, a complete union of the fragments always took place, irrespective of the treatment given.

ZUSAMMENFASSUNG

In einem Totalmaterial von 1 668 Kindern mit Fuss- und Fussgelenksverletzungen fand man 66 Frakturen an der Tuberositas ossis metatarsale V, die mit Hinsicht auf ihre Frequenz, Typ und Heilungsverlauf näher studiert wurden. Die Querfrakturen und die kleinen Ab-

sprengungen waren u. a. durch einen, dem Normalen gegenüber verlängerte Heilungsdauer charakterisiert. Ihre Prognose ist jedoch gut, da schliesslich bei allen diesen Frakturen, unabhängig von der Behandlungsmethode, komplette Heilung konstatiert werden konnte.

RÉSUMÉ

Sur un matériel total de 1 668 cas de traumatismes du pied et de la cheville chez des enfants, l'auteur a étudié, au point de vue de leur fréquence, de leur type et de leur mode de guérison, soixante-six fractures de la tubérosité du cinquième métatarsien. Les fractures transversales et les arrachements se sont tous caractérisés par un temps de guérison prolongé. Finalement, cependant, l'union complète des fragments se fit toujours, quel qu'ait été le traitement.

REFERENCES

BAASTRUP, CHR. I.: Os Vesalianum tarsi and fracture of tuberositas ossis metatarsi V. Acta radiol. 1 (1922), 334.

BLOUNT, W. P.: Fractures in children. Williams & Wilkins, Baltimore 1954.

BÖHLER, L.: Technik der Knochenbruchbehandlung. Bd. II, 2. Teil. Maudrich, Wien 1957.

CHIGOT, P. L. et ESTÈVE, P.: Traumatologie infantile. Expansion Scientifique Française, Paris 1958.

EHALT, W.: Unfallchirurgie im Röntgenbilde. Maudrich, Wien 1950.

ISELIN and SCHOUWEY: cit. by BAASTRUP.

JOHANSSON, S.: Os Vesalianum pedis. Z. orthop. Chir. 42 (1922), 301.

LANZ, T. und WACHSMUTH, W.: Praktische Anatomie, Bein u. Statik. Springer, Berlin 1938.

PFITZNER: cit. by BAASTRUP.

PREISS, G. A.: Knochenbruch und Knochenbruchheilung. *In*: Lehrbuch der Röntgendiagnostik. Bd 1, S. 304. SCHINTZ et coll. Georg Thieme, Stuttgart 1950.

RAUBER-KOPSCH: Lehrbuch und Atlas der Anatomie des Menschen. Georg Thieme, Leipzig 1947.

RETTIG, H.: Frakturen im Kindesalter. J. Bergmann, München 1957.

WENTZELGRUBER: cit. by BAASTRUP.

ZIMMER, E. A.: Grenzen des Normalen und Anfänge des Pathologischen im Röntgenbilde. Georg Thieme, Stuttgart 1953.

CONTRAST MEDIA

BILIJODON-NATRIUM [1]
(Sodium Salt of Iopanoic Acid USP XV)

An oral cholecystographic medium
- with high iodine contents
- is rapidly and completely absorbed
- gives a superior contrast
- gives no confusing colon shadows
- gives minimal side effects

NEW! BILIJODON CAPSULES
A new potent agent designed for
- oral cholegraphy

DIJODON [2]
(Diethanolamine Salt of Diodon)

A well-known contrast medium for
- urography
- urethrocystography
- hysterosalpingography
- arteriography
- phlebography
- aortography
- arthrography

DIJODON D
(Dijodon + 1 mg. Desentol per ml.)

Especially for
- urography
- discography

KONTRAST U
(Methiodal Sodium USP XV)

A contrast medium for
- myelography
- urethrocystography
- retrograde pyelography
- vasography
- cholangiography
- sialography

TRIUROL [3]
(Sodium Acetrizoate USP XV)

An intravascular contrast medium
- with high iodine contents
- of a low systemic toxicity
- gives a superior contrast
- is rapidly excreted
- gives minimal side effects

On certain markets: 1) Bilijodon, Panjopaque
2) Diodon, Diodon D 3) Trijodyl

LEO | HELSINGBORG SWEDEN

ACTA RADIOLOGICA

FOUNDED 1921 BY GÖSTA FORSSELL

is a monthly journal which publishes original articles in English, French, or German, in the fields of medical radiology and nuclear medicine, all articles being provided with summaries in all three languages. It is issued in two volumes a year, each volume of about 500 pages being published in six richly illustrated numbers.

Published and owned by

The Societies for Radiology of Denmark, Finland, Norway and Sweden

Printed in Sweden

EDITOR: ERIK LINDGREN

Editorial office, Administration and Sales department:

ACTA RADIOLOGICA

P. O. BOX 2052, STOCKHOLM 2, SWEDEN

Subscription rates:

per volume Sw Kr 40:—, annually Sw Kr 80:—, postage additional outside Scandinavia per volume Sw Kr 3:—, annually Sw Kr 6:—

Complete volumes

are still available for the years listed below and at the prices given:

Vols 4—22	Vols 23—27	Vols 34—39	Vols 41—53
(1925—1941)	(1942—1946)	(1950—1953)	(1954—1960)
Sw Kr 25:—	Sw Kr 30:—	Sw Kr 35:—	Sw Kr 40:—

The following volumes are out of print

Back numbers of some of the separate numbers are however still obtainable at a price of Sw Kr 7:— per copy as enumerated below:

Numbers:	1	2	3	4	5	6
Vol. 1 . . .	23	9	30	—	—	—
» 2 . . .	—	11	—	—	—	—
» 3 . . .	32	—	—	7	9	19
» 28 . . .	5	5	13	8	—	—
» 29 . . .	—	—	—	14	3	—
» 30 . . .	—	—	—	—	—	—
» 31 . . .	—	11	12	29	—	—
» 32 . . .	3	←2→		—	←12→	
» 33 . . .	—	—	—	—	—	—
» 40 . . .	—	←20→		31	54	37

Figures between arrows indicate double-numbers of respective issues.

FROM THE ROENTGENDIAGNOSTIC DEPARTMENT (DIRECTOR: PROF. OLLE OLSSON), THE INSTITUTE OF PATHOLOGY (DIRECTOR: PROF. C. G. AHLSTRÖM), AND THE DEPARTMENT OF THORACIC SURGERY (DIRECTOR: OLLE DAHLBÄCK), UNIVERSITY OF LUND, SWEDEN

EXPERIMENTAL PULMONARY EDEMA

by

KARL-ERIC BORGSTRÖM, ULLA ISING, ERLAND LINDER and ANDERS LUNDERQUIST

Roentgen examination plays an important role in the diagnosis and differential diagnosis of pulmonary edema of different types. Especially in the pulmonary edema in uremic patients, the diagnosis is mandatory. The first roentgenologic description of this type of edema in uremic patients was given by ROUBIER and PLAUCHAU (1934). Contributions by many authors, since then (HODSON 1950, SCHINZ et coll. 1952, ZALDIVAR & FARIÑAS 1954, OLSSON 1954), have clearly distinguished it from congestive pulmonary changes in heart failure.

The uremic pulmonary edema is characterized by central changes, surrounded by a free peripheral zone of normal lung parenchyma, 2 to 4 cm in thickness and slightly broader at the lobe limits (Fig. 1). It has been called 'butterfly edema' or 'bat's wing shadow edema'. Such pictorial names obviously do not belong in scientific radiology, and in this case do not correspond to the most characteristic roentgenologic feature, i. e. the central location of the changes, which are very marked in the hilar region around the tracheal bifurcation and corresponding parts of the esophagus. The initial changes are therefore usually best demonstrated in a lateral view. The heart size is often normal.

Submitted for publication 22 March 1960.

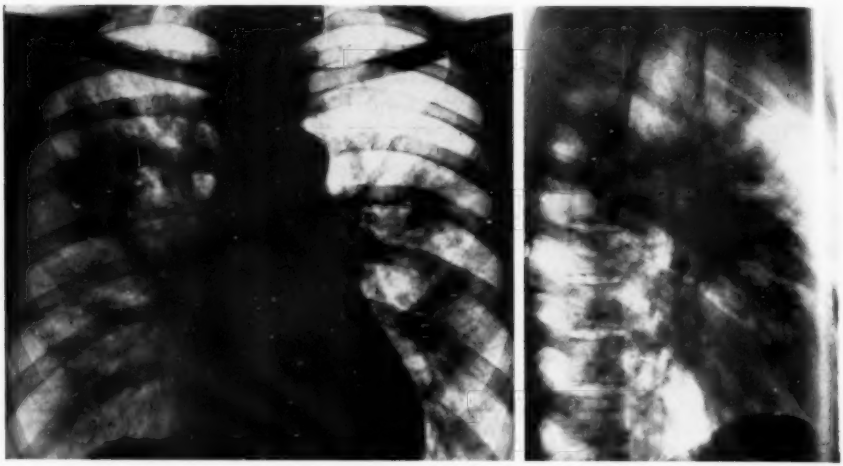

Fig. 1. A 37-year-old man, with advanced uremia. Typical pulmonary changes. Marked hilus changes and free peripheral zone.

The pulmonary edema in uremia may develop in the course of 24 to 48 hours, and be massive, and by appropriate therapeutic measures the regression of the pulmonary changes can be just as rapid.

The clinical symptoms and signs of non-complicated uremic pulmonary edema are few, if any, in spite of the marked roentgenologic lung changes (BASS and SINGER 1950, and others). This may be illustrated by a recent case.

A 42-year-old man (Rtg journal Pm 5093 var/1959), with arterial hypertension and proteinuria, became acutely ill with a sore throat and developed increasing renal insufficiency. On admission ten days later NPN was 224 mg %. Roentgen examination of the chest revealed marked uremic pulmonary edema but the patient showed no respiratory symptoms at that time (Fig. 2).

To compare with the above mentioned case, the chest roentgenogram of a 51-year-old woman (journal 080126/1959), is shown in Fig. 3. The patient developed acute pulmonary edema during the induction stage of anaesthesia for mitral commissurotomy. On opening the left thoracic cavity the left lung was firm and grossly consolidated, and frothy fluid escaped from the tracheal tube. Roentgen examination immediately after the operative procedure showed moderate diffuse edema in both lungs, involving the entire lungs, even the peripheral parts.

Most authors claim that left heart failure is the essential etiologic factor in the development of the uremic pulmonary edema (ROUBIER & PLAUCHAT 1934, KLIMA & ROSEGGER 1936, LELONG & BERNARD 1937, DONIACH 19[illegible]

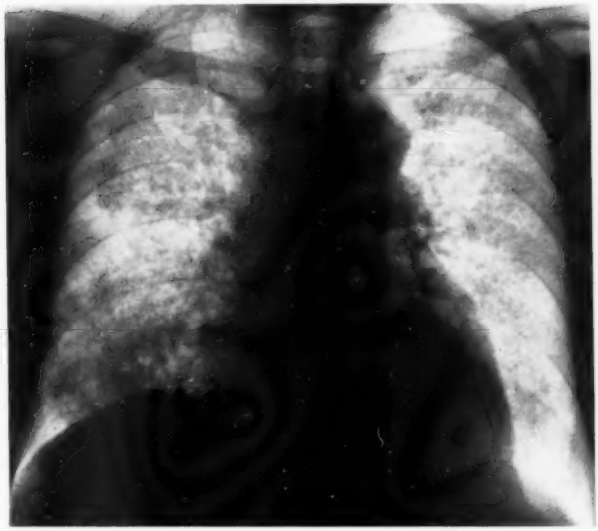

Fig. 2. A 42-year-old man, with arterial hypertension and proteinuria, after 10 days of progressive uremia.

and JACKSON 1951). A smaller group of investigators are doubtful about left heart failure as being the primary cause (GOODRICH 1948, DAVIS 1951, DE FAZIO et coll. 1959). The latter reported upon thorough hemodynamical studies, in seven cases of acute glomerulonephritis, but unfortunately they did not present any roentgenograms to substantiate pulmonary changes.

Left heart insufficiency is thought to be secondary to the fluid retention in uremia. In support of this view reference has been made to both experimental and clinical investigations in which large amounts of fluid have been given parenterally, and as a consequence pulmonary edema and signs of heart insufficiency have developed. In all experimental studies, the pulmonary changes with one exception (ALWALL, LUNDERQUIST & OLSSON 1953), have not been diagnosed roentgenologically. Furthermore, large amounts of fluid were infused, and the time of administration was very short (COHNHEIM & LICHTHEIM 1877, MORTHON 1935, CUTTING et coll. 1939, YEOMANS et coll. 1943). In clinical investigations, overhydration of patients with renal insufficiency has been shown to initiate pulmonary edema, while dehydration produces regression (NESSA & RIGLER 1941, RENNAES 1948, GOODRICH 1948, ALWALL et coll. 1949, 1953). These last mentioned authors (ALWALL et coll. 1953), found it worth-while to stress the role played by the excess of fluid

Fig. 3. A 51-year-old woman. Acute pulmonary edema during mitral commissurotomy. Very marked changes in the apical part of the left lower lobe.

and proposed to term the pulmonary changes 'fluid lung' (waterlogged lung). Referring to the experimental studies by LUNDERQUIST, OLSSON (1954) stated that there is a straight correlation between the degree of fluid retention and the severity of the pulmonary edema.

Several authors have suggested, as a cause of pulmonary edema, the presence of some toxic agent that could produce damage to the capillaries and thus alter the permeability. CAMERON & COURTICE (1946) produced pulmonary edema in rabbits by phosgene inhalations. They found the protein content of the edema fluid to correspond to the content in the blood plasma. LATTA (1947) and DRINKER & HARDENBERG (1949) produced edema by the poisoning of rats and dogs with intravenous and intraperitoneal injections of alpha-naphtylthiourea (ANTU). MOON and MORGAN (1936) showed that intravenous administration of sodium glychocholate in dogs produced lethal pulmonary edema in the course of some hours.

Even in man toxic capillary damage has been suggested as the cause of uremic pulmonary edema. EHRICH and MCINTOSH (1932) proposed this theory based on three cases of bronchiolitis obliterans diagnosed at autopsy of patients who died of Bright's disease. BARDEN & COOPER (1948) included this 'uremic pneumonia' as one of the groups associated with increased vascular perme-

al ity of the lung, along with such conditions as acute rheumatic fever, lu is erythematosus, periarteritis nodosa, etc.

onvincing evidence that altered permeability plays a dominant role in th pathogenesis of the uremic pulmonary edema has still not been produced.

he histo-pathologic verification of damage to the lung capillaries on bi psy material is difficult. Reported examinations have been performed on au psy specimens, but are complicated by terminal conditions (heart insu ciency, infections) and post mortem changes.

Anatomical considerations of the location of pulmonary edema

With the typical roentgen changes of uremic pulmonary edema as a starting point, MARCHAND (1951) on the basis of anatomical studies proposed that the location and appearance practically corresponded to the region in which the bronchi and pulmonary vessels are accompanied by extensions from the mediastinal fascia. This seems improbable because these extensions do not reach farther than to the third bronchial division but the lung changes extend far beyond these limits.

An attempt was made to explain the changes anatomically by HERRNHEISER & HINSON (1954) and HERRNHEISER (1955). According to their view the uremic pulmonary edema is localized to the 'medullary region' of the lobes of the lung. In the periphery of the lobe, which they termed 'cortex', there are mostly well-developed lobuli in one or two layers where no changes could be found. In the medullary part the lobuli are smaller in size and less numerous but the bronchi and vessels increase in diameter. The pulmonary artery divides into branches of the same diameter, but from these, smaller caliber branches are given off to the lobuli in the medulla as well. This was thought to be an anatomical foundation for the extension of the uremic pulmonary edema. They did not discuss the edema from a patho-physiologic point of view.

Many clinical observations strongly indicate the occurrence of some type of toxic damage in the systemic capillaries. As the bronchial circulatory system is a part of the systemic circulation this toxic factor might affect it. The bronchial arteries run adjacent to the bronchi from the hilum to the bronchioli respiratorii, and thus they do not supply the 2 to 4 cm thick peripheral zone (MILLER 1943). Disturbances in the permeability of the vascular region of the bronchial arteries might explain the pathogenesis of pulmonary changes in uremia, as well as their typical roentgenographic appearance. The possible importance of the bronchial circulatory system in the pathogenesis of pulmonary edema appears to have been discussed only by BRUNER & SCHMIDT (1947). They considered that an increase in the flow through the bronchial arteries might produce pulmonary edema by overtaxing the capacity of the pulmonary veins. On measuring the normal bronchial arterial flow they found it to be only about 1 % of the cardiac output and accordingly concluded

that an increase in bronchial arterial flow by 5 or 6 times is unlikely to overtax the drainage capacity of the pulmonary veins.

There is a striking similarity between the area of supply of the bronchial arteries and the extent of the roentgenologic changes in uremic pulmonary edema. A theory is put forth by the present authors that the primary cause of pulmonary edema in uremia be damage by toxins on the bronchial vessel walls, causing permeability disturbances, with consequent edema formation.

Anatomy of the bronchial vessels

STITZ 1936, LIEBOW et coll. 1950, HORINE & WARNER 1932, and NORDSTRÖM 1954, and others, have described the anatomy of the bronchial vessels in the dog. We have based our investigation on the anatomical descriptions published by these authors.

The bronchial arteries arise mainly as branches of the intercostal arteries, internal mammary arteries and directly from the aorta. The first branch of the right 6th intercostal artery was found to be the most constant, occurring in 60 % of the dogs studied. The bronchial arteries enter the region of the hilum, extend along the walls of the bronchi and terminate at the bronchioli respiratorii. MILLER believes that the pleurae are supplied predominantly by the pulmonary vessels. It has been demonstrated that the bronchial arteries also form the vasa vasorum of the pulmonary arteries and the pulmonary veins. The venous return of the blood from the bronchial arteries in the central part of the lung drains via the bronchial veins to the right side of the heart, and from the peripheral part by joining the pulmonary capillaries, and thus into the pulmonary veins.

In principle, the intrapulmonary bronchial arterial supply in human beings is similar to that found in dogs. In human subjects it has been shown (MILLER) that the bronchial arteries supply the mediastinal and interlobar pleura. The remaining pleura is supplied by the pulmonary arteries.

Material and Methods

Sixteen mongrel dogs, weighing between 13 and 32 kg, were used in these experiments. The dogs were anesthetized with 0.03 g per kg nembutal intravenously. Supplementary doses of 0.06 to 0.12 g nembutal were administered periodically during the course of the experiments. Endotracheal intubation was done routinely. In two dogs, where technical difficulties prolonged the procedure, artificial respiration was administered. A Cournand catheter 10 F was introduced into the aorta via the femoral artery. The experiments were performed by three different methods.

Group I. Induced alteration of the permeability of the bronchial capillaries. 11 dogs were used. An extra pleural approach was employed to expose the right 6th

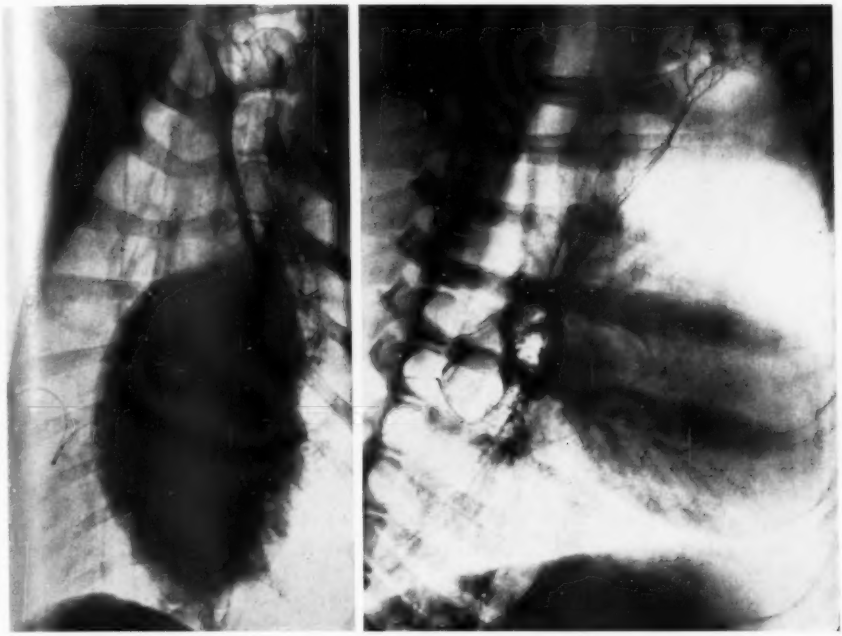

a b

Fig. 4 (dog 3). a) Angiography through the catheter inserted in the right 6th intercostal artery: filling of the bronchial vascular supply to the left apical lobe and both the right and left diaphragmatic lobes. b) Lateral projection: both arterial and venous filling was obtained.

intercostal artery. This was accomplished through an 8 to 10 cm long posterolateral incision at the level of the 6th intercostal space. A polythene catheter (P 20—50) was introduced into the intercostal artery at the level of the posterior axillary line and passed in a retrograde fashion to a point about 2 cm distant from the aorta. In all cases the heparinized catheter remained in the intercostal artery, and the incision was sutured around it. Arterial spasm was avoided by injection in the catheter of small amounts of an ergotamin preparation (Hydergin, Sandoz). Conditions were checked by angiography using 2 to 5 ml of Hypaque 45 % (sodium salts of 3.5-diacetylamino-2,4,6-triiodobenzoic acid) or Urografin 60 % (sodium salt and methyl glucamine salt of 3.5-diacetylamino-2,4,6-tri-iodobenzoic acid) (Fig. 4). In a few cases, Urografin 76 % was employed. The contrast injections were performed by hand and single exposures were obtained. It was found in the angiographic examinations that in six cases the bronchial artery arose from the right 6th intercostal

artery whereas in the remaining five cases no bronchial artery arose at this level. In these cases, a catheterization and a single exposure at the level of the 5th intercostal artery were performed, and in all cases a bronchial artery was found. At this point, control chest roentgenograms were obtained in a. p. and lateral projections. One or two Cournand catheters, number 7 F or 9 F, were inserted via the jugular veins through the right heart into the pulmonary artery. In the cases where two catheters were employed, one was wedged in a pulmonary artery branch. In the cases where only one catheter was used the catheter was repositioned intermittently between the pulmonary artery and a wedge position. Pressures were recorded with Elema strain gauge manometers, on a 2-channel direct writing oscillograph. The table top was designated as the zero point. A midline abdominal incision was then made and the ureters were ligated transperitoneally at the level of the pelvic inlet. It is important to ensure that all kidney drainage has ceased, by demonstrating roentgenologically that the presence of such anomalies as horse-shoe kidney or a double ureter can be excluded. This was readily accomplished because the contrast medium injected for angiography was excreted by the kidneys.

Pressure recordings were made, and roentgenograms of the chest were obtained after the surgical procedures in order to be sure that no significant change had occurred.

Bile-salts may produce pulmonary edema (MOON & MORGAN 1936); they have also been found to be potent substances in breaking down the blood-brain barrier (BROMAN & LINDBERG-BROMAN 1945). Therefore sodium-desoxycholate (SDO) in 0.2 to 0.8 % solution was chosen by us to produce increased permeability of the vascular system. Dosages varying from between 10 and 55 ml were injected through the catheter into the intercostal artery during 20 to 60 seconds. In 5 cases, the injection was repeated. An angiographic control was made immediately following each injection.

Nine dogs were made hypervolemic by intravenous administration of warm saline solution, given intermittently in an amount of 10 % of the bodyweight. In the remaining two animals no fluid was given.

Group II. Induced alteration of the permeability in the pulmonary capillaries. This group comprises 2 dogs. They were catheterized in the same fashion as described in the foregoing group except that no catheter was inserted in the intercostal artery. In one dog the ureters were ligated, and a volume of physiological saline, calculated at 6 % of the bodyweight, was administered intermittently in 40 minutes. Pressure recordings and chest roentgenograms were obtained as in group I. Through one of the catheters positioned in the pulmonary artery, SDO in 0.4 to 0.8 % solution was infused over a period of 30 to 55 seconds. The amount injected varied between 80 and 185 ml. The larger dosages in those dogs were chosen in order to compensate for the greater

blood flow in the pulmonary artery compared to the blood flow in the bronchial artery. During the infusions, the tip of the catheter was positioned so that no more than one lobe or part of one lobe was perfused at one time. Without changing the position of the catheter the perfused part of the lung was examined angiographically. After repositioning the catheter, the manoeuvres were repeated.

Group III. Induced left heart failure. In a single animal, catheterized in similar fashion as previously described, a catheter with an inflatable balloon at the tip was passed through the left common carotid artery and positioned in the descending aorta. The ureters were ligated, and physiologic saline, in an amount calculated at 10 % of the bodyweight, was infused intravenously. The balloon catheter was inflated to a volume sufficient to either partially or totally occlude the aorta at various levels of the descending aorta from the arch to the diaphragm. In order to place a greater load on the left ventricle, 1 mg of adrenaline was administered intravenously, divided into two dosages of 0.5 mg. In addition, 5 mg of noradrenaline in 1 000 ml of saline was administered intravenously.

Finally the right common carotid artery was ligated.

At the termination of the experiments the anesthetized animals were killed by exsanguination. A suspension of colloidal barium sulphate (Collobar Astra) was injected through the catheter into the intercostal artery of the first group. The chest was opened in all the dogs, and the lungs removed, reinflated and examined roentgenographically. Both lungs were fixed in 10 % formaldehyde, and specimens from the central and peripheral areas were obtained and prepared for microscopical examination.

Roentgen technique. All exposures were performed on a Bucky table employing a vertical beam. The endotracheal tube was clamped after a normal inspiration during the exposures. Focal spot 2 × 2 mm, FFD 122 cm, movable secondary diaphragm, exposure: 0.03 sec, 500 mA, 80 to 105 kV. Contrast medium, see preceding section. In each experiment, about 30 roentgenograms were produced.

Results

Of the 11 dogs in group I, two expired before the administration of the SDO. Angiographic studies of 3 dogs showed that the intrapulmonary bronchial arteries had become thrombosed, probably by the injection of a too high concentration of SDO. In the remaining 6 dogs pulmonary edema was successfully obtained. The two dogs in group II both developed pulmonary edema in the segment into which the injection was made. The dog in group III also manifested pulmonary edema roentgenographically. Although all the three types of experiments resulted in pulmonary edema, the roentgenographic features of each series differed markedly.

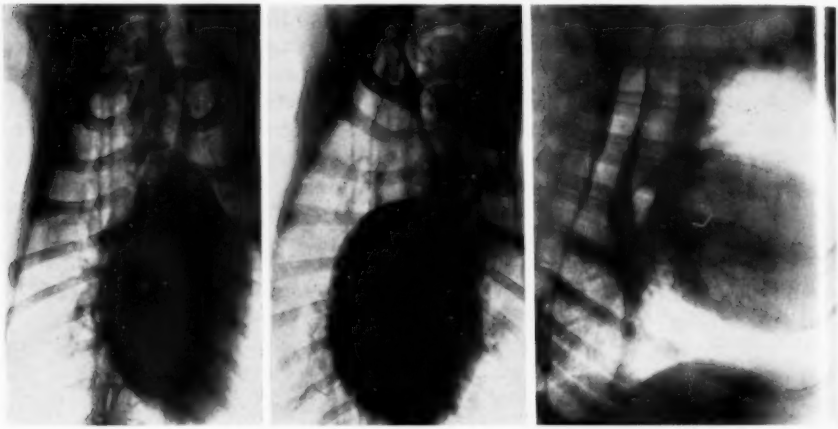

a b c

Fig. 5 (dog 3). a) Normal frontal roentgenogram before bronchial capillary damage. b) Bronchial capillary edema in the left apical lobe with a peripheral free zone. c) Marked central edema seen even in the tracheal and esophageal walls.

Bronchial capillary edema

An experimentally altered permeability in the bronchial circulation results in pulmonary edema of a typical roentgenographic appearance, which we have termed 'bronchial capillary edema'.

The edema is located in the central parts of the lung and is especially marked in the hilar region. This is best seen in a lateral projection. Even the adjacent parts of the esophagus and trachea are involved in the edema formation (Figs 5, 6, 7).

The edema extends along the bronchi and branches of pulmonary arteries and veins, but leaves the peripheral alveolar layers free. The first roentgenologic signs of this type of edema are the above mentioned changes in the region of the hilum. In all dogs, in which edema was demonstrated roentgenologically, there was a striking correlation between its location and the regions supplied by the injected bronchial arteries (Fig. 7f). No changes appeared in those regions where the permeability in the bronchial circulation was unaltered. No significant increase in heart size was recorded.

During the development of the edema, and even when it had reached its maximum, frothy fluid was not present in the respiratory tract, nor were any changes noted in the respiratory and heart rates.

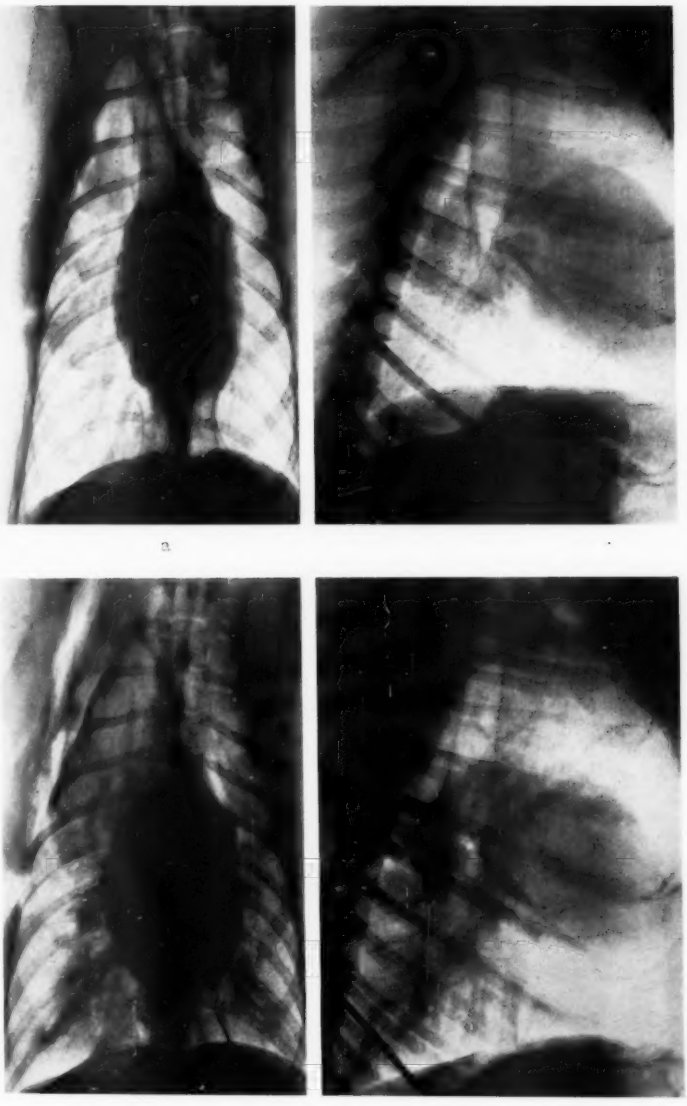

Fig. 6 (dog 6). Bronchial capillary edema. a) and b) Normal roentgenograms before bronchial capillary damage. c) and d) Massive central edema in both lungs. Heart size unchanged.

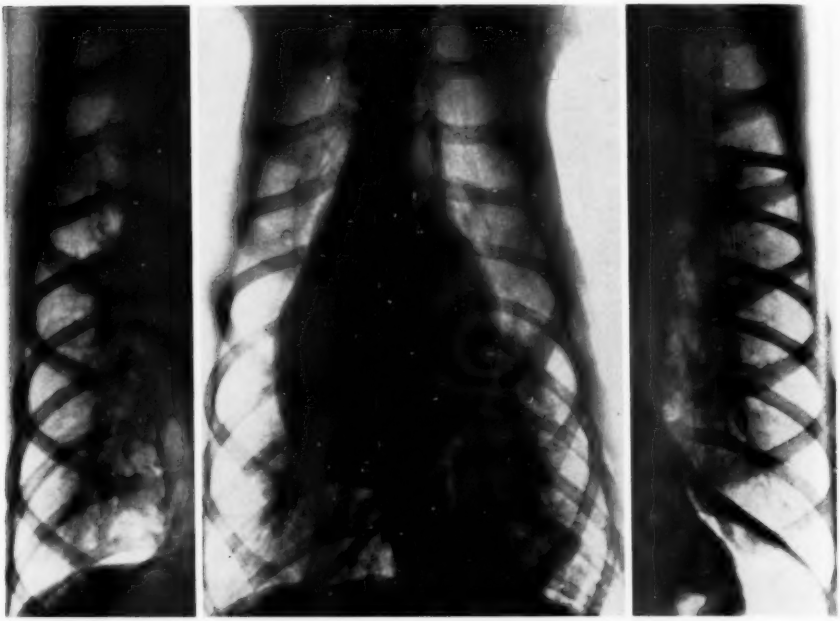

a b c

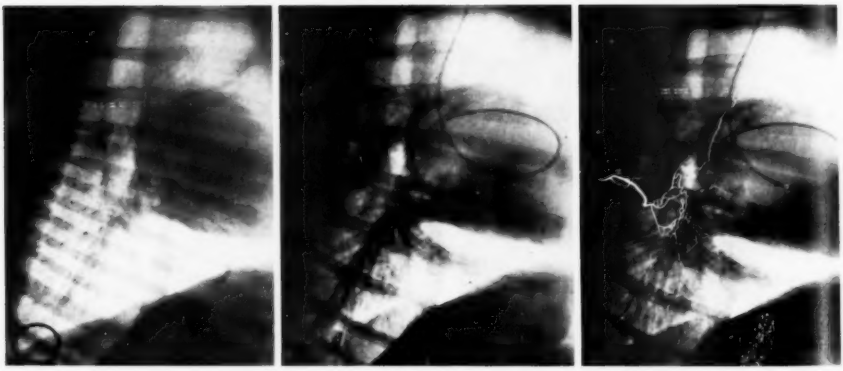

d e f

Fig. 7 (dog 11). Bronchial capillary edema. a), b) and c) Central edema in both lungs; the free zone in the periphery is well seen in the oblique projections. d) Normal lateral view before bronchial capillary damage. e) Marked central type of edema. f) Edema location corresponds to the affected bronchial arteries (schematic drawing from the angiogram is superimposed on the roentgenogram).

Autopsy findings

In 5 of the animals that developed edema, pleural effusion was found at autopsy in an amount of 30 ml or less. In the remaining dog, 100 ml of fluid were collected. The edema formation in the lungs of this dog was considerable bilaterally (Fig. 7).

All the dogs had mediastinal edema, and in 3 this was massive with involvement of the lung pedicles, the esophagus, and the region of the tracheal bifurcation.

The lungs felt solid in regions which roentgenologically showed in vivo edema. In the dog with bilateral edema the ratio of lungweight to bodyweight was 14.4 g/kg. Corresponding values were found by HARRISON & LINDBOW (1954) in dogs with slight pulmonary edema. In the other cases, this ratio was lower, which might be due to the fact that only those parts of the lungs were edematous that corresponded to the injected bronchial capillary region.

The small bronchial arteries were blood-filled and distended. Patchy hemorrhages were seen close to some of them (Fig. 8a).

The peribronchial tissue and perivascular areas around the pulmonary artery branches are swollen and separated by low protein-containing fluid. Adjacent alveoli are included in these edematous changes (Fig. 8, b and c). Scattered polymorphonuclear cells, indicating slight inflammatory reaction, Fig. 8d, are found in these edematous regions. No changes were seen in sections from the lung periphery.

Pulmonary capillary (alveolar) edema

In Fig. 9, c and e, the typical roentgenologic appearance is seen of the edema following SDO injection into a basal branch of the left and apical branch of the right pulmonary arteries which we have termed 'pulmonary capillary (alveolar) edema'. The location of the edema corresponds well to the preceding selective angiogram (Fig. 9b). This strictly confined edema extends through the periphery with unchanged intensity. The heart size is normal.

During the injection of SDO, frothy fluid began to escape through the tracheal tube and soon overflowed, which necessitated endotracheal suction. The respiratory rate was markedly increased. At autopsy, no pleural effusion was present. In the region where SDO had been injected, the lung parenchyma was consolidated and showed multiple subpleural hemorrhages.

In sections from both the central and peripheral parts of the macroscopically edematous lung segments almost all alveoli were filled with protein-rich and cell-free fluid (Fig. 10). The capillaries at the alveolar walls were markedly distended and blood-filled, and fresh hemorrhages appeared within several alveoli. There was no significant peribronchial or perivascular edema, and inflammatory cells were absent.

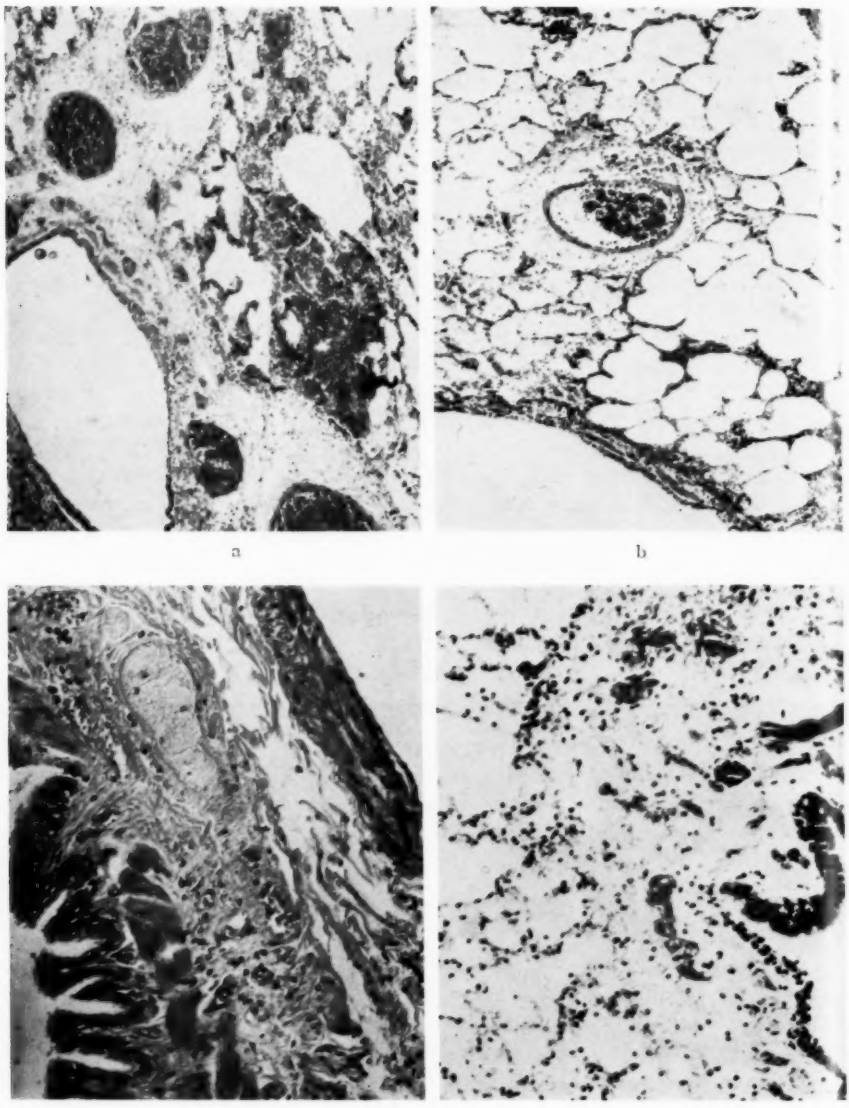

Fig. 8. Bronchial capillary edema. a) The small bronchial arteries are blood-filled and distended. Patchy hemorrhages close to some of them. × 83. b) and c) The peribronchial tissue and perivascular areas around pulmonary artery branches are swollen and separated by low protein-containing fluid. Adjacent alveoli are included in these edematous changes. × 83, and × 210, respectively. d) Scattered polymorphonuclear cells are seen in the edematous regions, indicating slight inflammatory reactions. × 200.

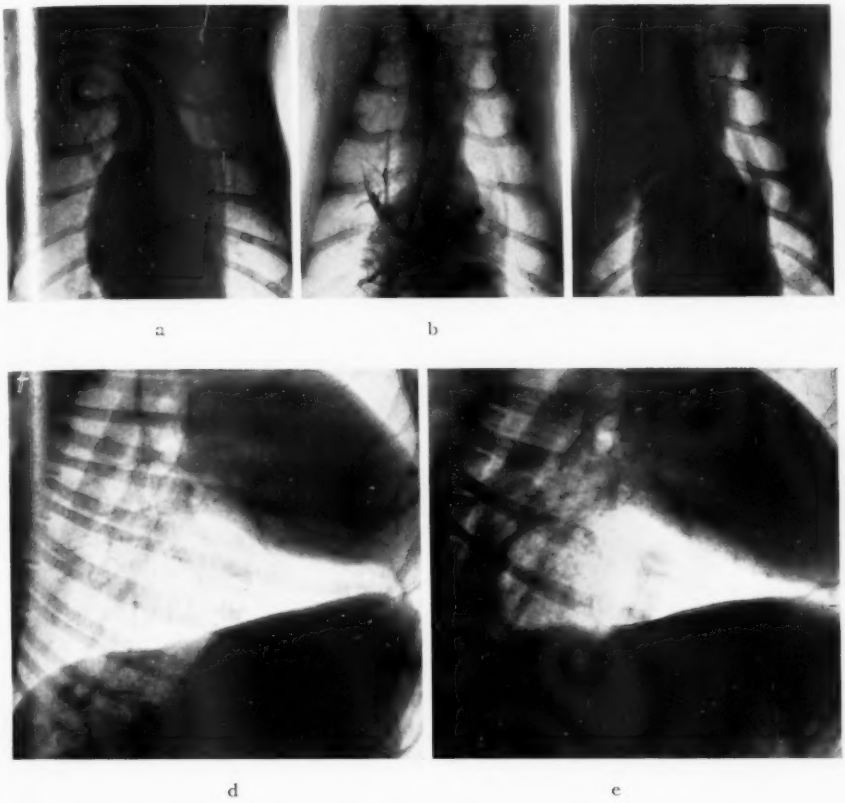

Fig. 9 (dog 12). Pulmonary capillary edema. a) Normal. b) Pulmonary angiography with predominant filling of the right apical lobe. c) Resulting massive edema which extends to the periphery. d) Normal. e) The same appearance of edema in one segment of the left diaphragmatic lobe with a different catheter position.

Left heart failure edema

The roentgen signs of edema resulting from left heart failure are demonstrated in Fig. 11. This edema is seen in the dorsal and basal parts of both lungs, with an increasing intensity towards the periphery. There are only negligible central changes, in contrast to the central predominance in 'bronchial capillary edema'. In cases with left heart failure, developing during a few hours, there is no obvious increase of the lung vascularity. The heart size on the other hand, increased conspicuously in the course of the experiment.

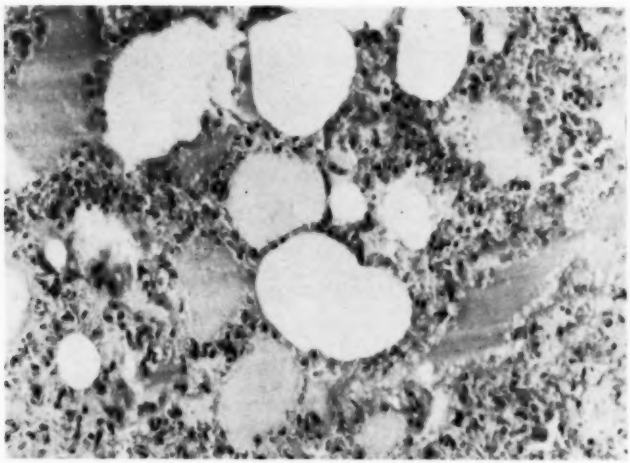

Fig. 10 (dog 12) (cf. fig. 9). Pulmonary capillary edema. Almost all alveoli are filled with protein-rich and cell-free fluid. × 210.

This dog, as well as all other dogs, was turned repeatedly from one position to another during the whole experiment to counteract hypostatic changes.

The clinical picture of severe acute pulmonary edema did not occur until one and a half hours after the first roentgenologic signs of lung changes. Profuse edema fluid was noted in the airways shortly before the spontaneous death of the dog.

Autopsy. A large amount of fluid was collected from the pleura. The lower lobes of both lungs were heavy, and abundant edema could be expressed from their cut surfaces. The apical lobes were more airfilled and less edematous.

Hemodynamic studies

When 'bronchial capillary edema' was found at the roentgen examination, hemodynamic studies were added to the experiments. Aside from the aortic pressure, the pulmonary artery and wedge pressures were studied only in 4 dogs of this group. In Fig. 12, uppermost diagram, are shown the various factors observed during a typical experiment. The pulse rate varied between 134 and 156 per min. The systolic and diastolic aortic pressures remained stable except for a transitory increase during the saline infusions, depending upon the increase in cardiac output. At 40 min after the first SDO injection the edema was demonstrable roentgenologically, but there was no elevation in the pulmonary artery pressure. This pressure rose 7 mm of Hg when 1 000 ml

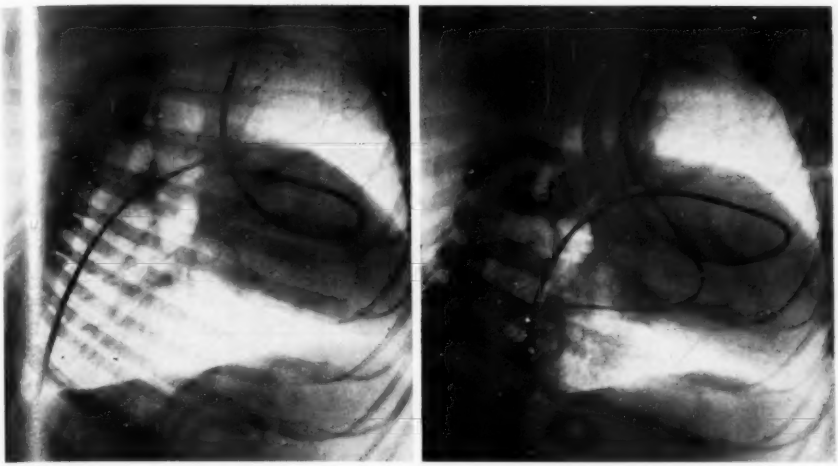

Fig. 11 (dog 13). Left heart failure edema. a) Normal. b) Peripheral alveolar edema chiefly in the dorsal, basal part of the diaphragmatic lobes. Marked increase of heart size.

of a physiologic saline solution was administered intravenously in 13 min, but returned to a normal level 10 min later. At this time the edema had increased roentgenologically, and 42 min later, when the edema was still more marked, the pulmonary artery systolic pressure had risen to 40 mm of Hg. During this part of the experiment the dog was artificially ventilated, but when allowed to breath spontaneously a slight drop in the pulmonary artery pressure was recorded. After repeated saline infusions intravenously, and another SDO injection into the bronchial arteries, there was a further elevation of the pulmonary artery pressure which was finally recorded at 62/48 mm of Hg. During the remaining 35 min, the pulmonary capillary mean pressure underwent only small variations within the upper limit of normal. Pressure recordings in a recent clinical case with uremic pulmonary edema showed similar findings (Fig. 2).

The pressure records of one of the two dogs in which 'pulmonary capillary edema' was produced are presented in Fig. 12, middle diagram. The rise in the pulmonary artery pressure after two saline infusions is also moderate and transitory in this dog. Unfortunately, no pressure recordings were made just previous to the first SDO administration into the basal branch of the left pulmonary artery. This was followed by a rapid development of the circumscribed edema in the left lower lobe (Fig. 9e) but 40 min later an unchanged pulmonary artery pressure was recorded. The second SDO-infusion, with a

Fig. 12

Bronchial capillary edema.

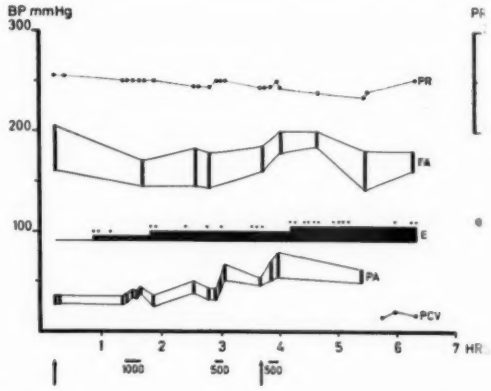

Pulmonary capillary (alveolar) edema.

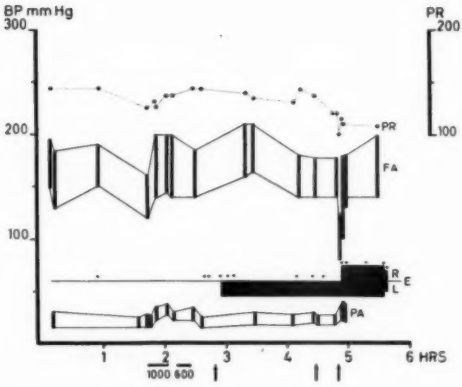

Left heart failure edema.

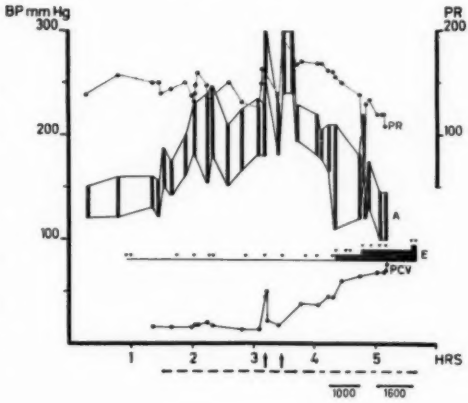

Definitions

Pulse rate (PR)

Systolic and diastolic pressures, in the femoral artery (FA), in the aorta (A)

Intensity of roentgenologic edema (E), in right (R) and left (L) lung

Roentgen exposure (V)

Systolic and diastolic pressures in the pulmonary artery (PA)

Pulmonary capillary mean pressure (PCV)

Top and middle diagrams: SDO injection (↑); Saline infusion (←→); Occlusion of the aorta (←– –→).

Lowermost diagram: Adrenalin intravenously (↑).

resulting massive edema in a larger part of the right lung (Fig. 9c) was associated with a dramatic fall in the aortic pressure and pulse rate, but there was a 13 mm increase in the pulmonary artery systolic pressure. In the second dog in this group the pulmonary capillary pressure was also recorded and found to be within normal limits.

The dog with the experimentally produced left heart failure (Fig. 12, lowest diagram) showed a marked rise in the aortic pressure, corresponding to the occlusion of the thoracic aorta at the level of the diaphragm. The second, still more marked pressure-rise resulted from a repeated and prolonged occlusion at the same level. This pressure-rise was accompanied by a slight increase of the wedge pressure, which returned to a normal value when the catheter balloon ruptured, as seen in the aortic pressure tracing. The occlusion was repeated after insertion of a new balloon catheter, which was positioned distally in the aortic arch. Despite a duration of 15 min of this occlusion, the PCV-pressure remained unchanged. To increase the load on the left heart, 0.5 mg adrenaline was given intravenously, with marked response both in aortic and PCV-pressures and increase in the pulse rate. A permanent rise in the PCV-pressure was obtained after a second injection of the same dosage of adrenaline. Just before roentgenologic signs of acute pulmonary edema appeared, a mean PCV-pressure of 44 mm Hg was recorded. A saline infusion containing norepinephrine was started. There was a steady increase in PCV-pressure and in the degree of the edema, resulting in progressive circulatory collapse.

Discussion

Our primary intention with the present investigation was to find an anatomical and pathophysiological basis for the specific roentgen findings in uremic pulmonary changes. By inducing an increased permeability in the bronchial circulation in dogs it has been possible to produce changes in the lungs with the following roentgenologic characteristics:

1. Central changes, with marked swelling of the bronchial walls and the walls of the pulmonary artery and vein branches.
2. Swelling of the esophageal and tracheal walls.
3. No involvement of the peripheral alveolar layers.
4. Little or no pleural effusion.
5. No increase of heart size.

These findings are characteristic of the changes seen at a roentgen examination of a patient with non-complicated uremic pulmonary changes. This is also in agreement with the clinical picture, in which respiratory symptoms and signs are faint or absent because the edema is interstitial. This is in contrast to the 'pulmonary capillary edema' and the lung changes in left heart

failure, where edema fluid appears in the airways. The latter types of pulmonary changes also differ in their peripheral location roentgenologically, when compared with the 'bronchial capillary edema'. The enlarged heart, in the condition of left heart failure, as well as the significant pleural effusion, are prominent findings on chest roentgenography.

It has thus been possible to produce both 'bronchial capillary edema' and 'pulmonary capillary edema' simply by altering the permeability in the corresponding capillary regions.

It is obvious from the above results that intravenous fluid administration alone, up to 10 % of the bodyweight, did not result in pulmonary changes detectable at chest roentgenography. On the other hand, hemodilution undoubtedly had a potentiating effect on the edema.

In the etiology of uremic pulmonary edema in man, hemodilution is considered to be an essential factor. Pulmonary edema may, however, develop or remain even if hemodilution is prevented or removed by dehydration therapy. In conformity with our findings in 'bronchial capillary edema' this observation in human subjects strongly suggests that altered permeability by some toxic agent is of prime importance in the development of uremic pulmonary edema. A basis for therapy in these cases might thus be a removal of this toxic factor.

Several investigators have produced experimental pulmonary edema by intravenous fluid administration alone. The course of this pulmonary edema has been assumed to be a sudden overloading of the left heart, with a resulting pressure-rise in the pulmonary capillaries. In our investigation, in which physiologic saline solution in an amount of 10 % of the bodyweight was infused, only slight and temporary elevation of the wedge pressure was recorded. Similar recordings were made from the pulmonary arteries. Signs of left heart insufficiency were not present. No significant changes were observed in this recordings even after several hours of anesthesia. During the development of 'bronchial capillary edema', however, hypertension developed in the pulmonary artery. This hypertension was not accompanied by an elevation of the pressure in the pulmonary capillaries. With unchanged pulse rate, and relatively stable arterial blood pressure, large variations in cardiac output might be excluded. Thus, there was a significant increase in resistance to the blood flow through the pulmonary artery. No final conclusions were reached about the cause of this increase in resistance from our present data, but it will be analysed in further investigations.

Conclusion. The present investigation indicates that a change in the permeability of the bronchial capillaries may be the prime etiologic factor in the production of uremic pulmonary edema. Consequently, a reduction in the osmotic pressure of the blood produced by overhydration, and/or a complicating left heart failure, act as enhancing factors.

SUMMARY

The roentgenographic appearance of uremic pulmonary edema is discussed and the localization of the changes to the central portion of the lungs are stressed. Different types of pulmonary edema were produced in dogs. An experimentally produced alteration of the permeability in the bronchial capillaries resulted in pulmonary edema which roentgenologically showed a striking similarity to uremic pulmonary edema in man. Hemodynamic studies and clinical observations suggest that altered bronchial capillary permeability resulting in pulmonary edema is secondary to the toxic action of uremia. Hemodilution and left heart insufficiency, when present, are complementary factors in the pathophysiology of uremic pulmonary edema.

ZUSAMMENFASSUNG

Das röntgenologische Aussehen des urämischen Lungenödemes wird diskutiert und die Lokalisation der Veränderungen, besonders in den zentralen Lungenabschnitten, hervorgehoben. Experimentell erzeugte Veränderungen der Permeabilität der Bronchialkapillaren resultierten in einem Lungenödem, welches im Röntgenbild eine starke Ähnlichkeit mit dem urämischen Lungenödem des Menschen zeigte. Experimentelle haemodynamische Studien und klinische Beobachtungen lassen vermuten, dass die veränderte Permeabilität der Bronchialkapillaren, die zum Lungenödem führt, eine Folge der toxischen Wirkung der Urämie darstellt. Hämodilution und linksseitige Herzinsuffizienz, falls sie vorhanden ist, ergänzen das pathophysiologische Bild des urämischen Lungenödemes.

RÉSUMÉ

Les auteurs décrivent les aspects radiologiques de l'œdème pulmonaire urémique et insistent sur la localisation des modifications dans la partie centrale des poumons. Différents types d'œdème pulmonaire ont été provoqués chez des chiens. La production expérimentale d'une altération de la perméabilité des capillaires bronchiques cause un œdème pulmonaire qui présente une similitude radiologique frappante avec l'œdème pulmonaire urémique chez l'homme. Les études hémodynamiques et les constatations cliniques font penser que l'altération de la perméabilité des capillaires bronchiques qui cause l'œdème pulmonaire est secondaire à l'action toxique de l'urémie. L'hémodilution et l'insuffisance du cœur gauche, quand elles existent, sont des facteurs adjuvants de la pathophysiologie de l'œdème pulmonaire urémique.

REFERENCES

ALWALL, N. and HERNER, B.: On the artificial kidney. VI. Acta med. scand. 132 (1949), 572.

— LUNDERQUIST, A. och OLSSON, O.: Uremi-lunga — vätske-lunga? (In Swedish.) Nord. med. 49 (1953), 211.

BARDEN, R. and COOPER, D.: The roentgen appearance of the chest in diseases affecting the peripheral vascular system of the lungs. Radiology 51 (1948), 44.

BASS, H. E. and SINGER, E.: Pulmonary changes in uremia. J. Amer. med. Ass. 144 (1950), 319.

BROMAN, T. and LINDBERG-BROMAN, A. M.: An experimental study of disorders in the permeability of cerebral vessels ('the blood-brain-barrier') produced by chemical and physicochemical agents. Acta physiol. 10 (1945), 102.

BRUNER, H. D. and SCHMIDT, C. F.: Blood flow in the bronchial artery of the anesthetized dog. Amer. J. Physiol. 148 (1947), 648.

CAMERON, G. R. and COURTICE, F. C.: The production and removal of oedema fluid in the lung after exposure to carbonyl chloride (phosgene). J. Physiol. (Lond.) 105 (1946), 175.

COHNHEIM, J. und LICHTHEIM, L.: Über Hydrämie und hydrämisches Ödem. Virchows Arch. path. Anat. 69 (1877), 106.

CUTTING, R. A., LARSON, P. S. and LANDS, A. M.: Cause of death resulting from massive infusions of isotonic solutions. Arch. Surg. 38 (1939), 599.

DAVIES, C. E.: Heart failure in acute nephritis. Quart. J. Med. 78 (1951), 163.

DEFAZIO, V., CHRISTENSEN, R. C., REGAN, T. J. et coll.: Circulatory changes in acute glomerulonephritis. Circulation 20 (1959), 190.

DONIACH, I.: Uremic edema of the lungs. Lancet 2 (1949), 911.

EHRICH, W. and MCINTOSH, J. F.: The pathogenesis of bronchiolitis oblitérans. Arch. Path. 13 (1932), 69.

GOODRICH, W. A.: Pulmonary edema. A correlation of X-ray appearance and physiological changes. Radiology 51 (1948), 58.

HARRISON, W. and LIEBOW, A. A.: The effects of massive intravenous infusions with special reference to pulmonary congestion and edema. Yale J. Biol. Med. 26 (1954), 372.

HERRNHEISER, G.: Zur Röntgendiagnostik des Lungenödems. Fortschr. Geb. Rtgstr. 89 (1958), 125.

— and HINSON, K. F. V.: An anatomical explanation of the formation of butterfly shadows. Thorax 9 (1954), 198.

HODSON, C. J.: Pulmonary oedema and the 'batswing shadow'. J. Fac. Radiol. 1 (1950), 176.

HORINE, C. F. and WARNER, C. G.: Distribution of the pulmonary and bronchial circulation; an experimental study. J. thorac. Surg. 2 (1932), 80.

JACKSON, F.: The radiology of acute pulmonary oedema. Brit. Heart J. 13 (1951), 503.

KLIMA, R. und ROSEGGER, H.: Eigenartige Krankheitsbilder zufolge von Lungenödem bei Niereninsuffizienz. Med. Klin. 32 (1936), 85.

KOENIG, H. and KOENIG, R.: Production of acute pulmonary edema by ammonium salts. Proc. Soc. exp. Biol. (N. Y.) 70 (1949), 375.

LATTA, H.: Pulmonary edema and pleural effusion produced by acute alpha-naphthyl thiourea poisoning in rats and dogs. Bull. Johns Hopkins Hosp. 80 (1947), 181.

LELONG, M. et BERNARD, J.: L'image radiologique d'un cas d'œdème aigu du poumon d'origine rénale chez un enfant. Soc. med. Hôp. Paris (1937), 177.

LIEBOW, A. A., HALES, M. R., BLOOMER, W. E. et coll.: Studies on the lung after ligation of the pulmonary artery. Amer. J. Path. 26 (1950), 177.

MARCHAND, P.: The anatomy and applied anatomy of the mediastinal fascia. Thorax 6 (1951), 359.

MILLER, W. S.: Key points in lung structure. Radiology 4 (1925), 173.

— The lung. Charles C. Thomas, Springfield, Ill. 1937.

MOON, V. H. and MORGAN, D. R.: Experimental pulmonary edema. Arch. Path. 21 (1936), 565.

NAIRN, R. C.: Oedema and capillary anoxia. J. Path. Bact. 63 (1951), 213.

NESSA, C. B. and RIGLER, L. G.: The roentgenological manifestations of pulmonary edema. Radiology 37 (1941), 35.

NORDENSTRÖM, B.: Temporary unilateral occlusion of the pulmonary artery. Acta radiol. (1954) Suppl. No. 108.

OLSSON, OLLE: Some radiological problems connected with Bright's disease. Brit. J. Radiol. 27 (1954), 86.

F NNAES, S.: On the roentgenological picture of pulmonary edema. Acta radiol. 30 (1948), 169.
F UBIER, C. et PLAUCHAU, M.: Sur certains aspects radiographiques de l'œdème pulmonaire chez les cardio-rénaux azotémiques. Arch. méd.-chir. Appar. resp. 3 (1934), 189.
S HINZ, H. R., BAENSCH, W. E., FRIEDL, E. und UEHLINGER, E.: Lehrbuch der Röntgendiagnostik, p. 2212. Georg Thieme Verlag, Stuttgart 1951.
S TZ, B.: Anatomische Untersuchungen über der Verlauf der Aa. und Vv. bronchiales des Hundes und über ihre Anastomosen mit dem Pulmonalgefässystem. Springer, Hannover 1936.
W ARTHEN, H. J.: Massive intravenous injections. Arch. Surg. 30 (1935), 199.
Y OMANS, A., PORTER, R. R. and SWANK, R. L.: Observations on certain manifestations of circulatory congestions produced in dogs by rapid infusion. J. Clin. Invest. 22 (1943), 33.
Z LDIVAR, R. A. G. e FARIÑAS, L.: Pulmon azotemico o edemea subagudo del pulmon en los renales. Rev. cubana Cardiol. 14 (1954), 141.

FROM THE DEPARTMENT OF RADIOLOGY (DIRECTOR: B. W. A. LEEMING), HUTT HOSPITAL, LOWER HUTT, NEW ZEALAND

TENDINITIS CALCAREA OF THE EXTENSOR ORIGIN AT THE ELBOW WITH EFFUSION OF THE JOINT

by

W. J. WESTON

Several cases of peritendinitis calcarea at the elbow have been reported in the literature but no associated effusion in the elbow joint has been described. NORELL (1954), in a paper on the visualization of the extracapsular fat, laid down the radiographic signs in the diagnosis of an effusion at the elbow joint. The purpose of this paper is to present a case of acute tendinitis calcarea at the extensor origin from the humerus, associated with an effusion in the elbow joint.

It is interesting to note that JONES (1955), when discussing acute episodes with calcification around the hip joint stated: 'The physical signs immediately after the onset of severe pain were those of an acute synovitis of the hip, movement being limited and painful in all directions, the hip being typically held in a little flexion abduction and lateral rotation. This suggests that the deposits ruptured into the hip joint rather than from tendon into soft tissues or into bursa. The material is extremely irritant and provokes a hyperaemic reaction with acute synovitis which facilitates its spontaneous absorption'.

It is suggested on the basis of the case here reported that a synovial effusion in the closely related joint is a feature of the acute case and not due to rupture of the calcareous material into the joint. The effusion and the subcutaneous oedema disappear as the acute phase settles.

Submitted for publication 15 December 1959.

a

b

c

Fig. 1. a) and b) Calcification at the extensor origin. The lateral view shows a large effusion in the elbow joint. c) Five weeks later the calcification has almost completely disappeared. No effusion.

Four cases of tendinitis calcarea at the elbow were found in the record of this department over a seven year period. Three of these were subacute in type and showed no evidence of a synovial effusion. One is reported upon in the following and illustrated in Fig. 1, a to c.

Case report. Mrs B. H., aged 35, a housewife, stated that her elbow had been very painful for 24 hours. No history of trauma. The maximum tenderness was over the head of radius and some swelling was present. Flexion and extension were considerably reduced. The pain about the elbow increased in intensity, and radiated into the hand which was cold and blue. The arm was elevated and kaolin plasters were applied hourly; Pethidine was used for relief of pain.

Laboratory investigations gave the following results: B. S. R. 27 mm/hour, haemoglobin 12.8 grampercent, white blood count 8 700 /mm³ (N 75 %, L 21 %, and M 4 %).

Five weeks later the elbow was comfortable during active movement but there was still local tenderness over the external epicondyle. The *roentgen* examination now showed almost complete clearing of the calcium salts and the effusion was no longer present (Fig. 1c).

SUMMARY

The author presents a case of tendinitis calcarea of the extensor origin at the elbow, associated with an effusion in the joint. The clinical picture was that of an acute arthritis.

ZUSAMMENFASSUNG

Der Autor zeigt einen Fall von Tendinitis calcarea an der Streckseite des Ellbogens in Verbindung mit einem Erguss im Gelenk. Das klinische Krankheitsbild war das einer akuten Arthritis.

RÉSUMÉ

L'auteur présente un cas de tendinite calcaire de l'insertion de l'extenseur au coude, associée à un épanchement dans l'articulation. Le tableau clinique était celui d'une arthrite aigüe.

REFERENCES

Cowan, I. I. and Stone, J. R.: Painful periarticular calcification at wrist and elbow. Diagnosis and treatment. J. Amer. med. Ass. 149 (1952), 530.

Fiorentini, A.: La periartrite calcarea del gomito. Arch. Ortop. 53 (1937), 385.

Gondos, B.: Observations on peritendinitis calcarea. Amer. J. Roentgenol. 77 (1957), 93.

Henrichsen, A.: Beitrag zur Diagnose der 'Kalkgicht'. Röntgenpraxis 1 (1929), 845.

Hughes, E. S. R.: Acute deposition of calcium near elbow. J. Bone Jt Surg. 32 B (1955), 30.

Jones, G. B.: Acute episodes with calcification around the hip joint. J. Bone Jt Surg. 37 B (1955), 448.

Key, J. A.: Calcium deposits in the vicinity of the shoulder and other joints. Ann. Surg. 129 (1949), 737.

Lapidus, P. W.: Infiltration therapy of acute tendinitis with calcification. Surg. Gynec. Obstet. 76 (1943), 715.

Norell, H. G.: Roentgenologic visualisation of the extracapsular fat. Its importance in diagnosis of traumatic injuries to the elbow. Acta radiol. 42 (1954), 205.

Sandström, C.: Peritendinitis calcarea. Acta radiol. 18 (1937), 263.

— Peritendinitis calcarea. Amer. J. Roentgenol. 40 (1938), 1.

Schmitt, J.: Bursitis calcarea am Epicondylus externus humeri. Arch. orthop. Unfall-Chir. 19 (1921), 215.

FROM THE ROENTGENDIAGNOSTIC DEPARTMENT (DIRECTOR: PROF. SÖLVE WELIN),
MALMÖ ALLMÄNNA SJUKHUS, MALMÖ, SWEDEN

INSTABILITY OF THE PUBIC SYMPHYSIS AND CONGENITAL DISLOCATION OF THE HIP IN NEWBORNS

The possible aetiologic role of maternal hormones

by

LARS ANDRÉN

It is widely believed that the primary cause of dislocation of the hip in newborns is congenital dysplasia of the joint. This concept has, however, not remained unchallenged. Thus, HOWORTH (1947), for example, writes: 'Dislocation could be due primarily to a relaxed capsule or to a deformity of the acetabulum. At operation, the capsule has always been found elongated, necessarily, but the acetabulum is frequently too well formed to justify the supposition that it is only a primary factor', and he adds 'it is likely that relaxation of the capsule is the primary factor'. He assumes at the same time that the relaxation of the capsule is a gradual process.

Relaxation of the capsule with dislocation of the hip-joint can be demonstrated at birth by the 'snapping' phenomenon (FROELICH 1911, LE DAMANY 1912, ORTOLANI 1935, and others). It has also been shown that every case of congenital dislocation of the hip can be diagnosed at birth by clinical as well as by roentgenologic methods (ANDRÉN & v. ROSEN 1958). Experimental dislocation in newborn rabbits (LANGENSKIÖLD & SARPIO 1957) and in puppies (SMITH et coll. 1958) is followed by typical dysplasia.

Submitted for publication 4 April 1960.

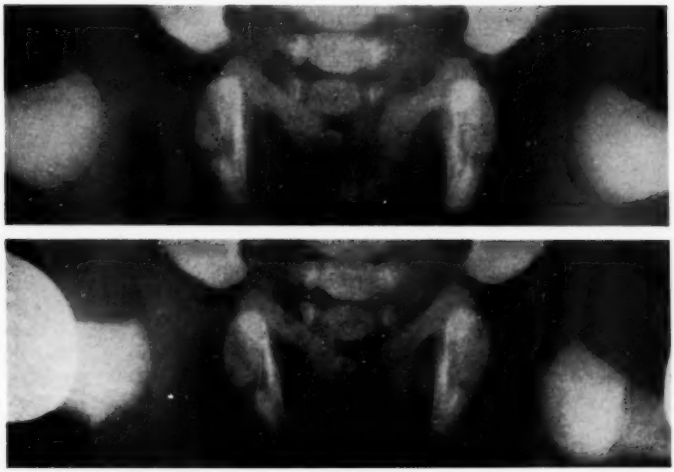

Fig. 1. *Upper*: Posterolateral dislocation of femoral heads, widening of symphysis. *Lower*: Femoral heads in acetabula. Decreased width of symphysis.

Personal observations. On roentgen examination in 1959 of a series of newborns with congenital dislocation of the hip, co-existent instability of the symphysis pubis was noticed. When the femoral head was pressed against the acetabulum and then dislocated posterolaterally, the manipulation was accompanied by a widening of the symphysis by 3 mm. A distinct relaxation of the capsule was observed, which stretched as the femoral head slipped out of the acetabulum (Figs 1 and 2).

Material

During the last 6 months, 3 cases of congenital dislocation of the hip have been seen at the hospital. All 3 patients were girls. They were examined on the first day of life for any such widening of the symphysis; the joint was found to widen from 4 to 7 mm, from 6 to 9 mm and from 3 to 6 mm in association with the examination. The difference in the distance between the femoral heads in the two positions was 10, 13 and 9 mm, respectively.

For comparison, 40 normal newborns (21 girls, 19 boys) were examined in a similar way: the femoral head was first pressed against the acetabulum and then pulled posterolaterally. The pull applied was stronger than that used in the girls with congenital dislocation of the hip. A distinct increase was observed in the distance between the posterior parts of the ischia (Fig. 3). In the majority of these controls the widening of the symphysis was less than

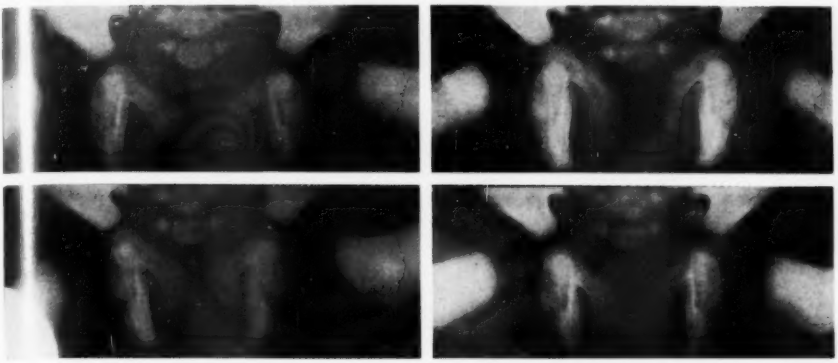

a b

Fig. 2. a) Same positions as in fig. 1. b) 8 days later. Only slight difference in width of symphysis. Hips could no longer be dislocated.

1 mm; only in two it was as much as 1.5 mm. The greatest difference in the distance between the femoral heads was 7 mm (average 4 mm).

Though the present series is as yet very small, it appears that the instability of the symphysis pubis, observed in all 3 patients studied, has something to do with the dislocation since the widening was unequivocal and so much greater than in the controls.

Discussion

Instability of the symphysis pubis is known to occur in pregnancy, physiologically, and particularly in so-called pelvic insufficiency. This instability is ascribed to an increased elaboration of oestrogens and of the pregnancy hormone, relaxin. Symphyseal instability has also been induced in animals by injection of large doses of oestrogen or relaxin. The degree of instability varies from one species to another and from animal to animal of the same species. The response is on the average more marked in females.

It is therefore tempting to assume that the symphyseal instability and relaxation of the capsule of the hip-joint are due to the influence of maternal hormones. CHAPPLE suggested this possibility in 1941, and later writes: 'In some instances there is a familial history of congenital dislocation of the hip. In such cases it is not known whether there is some genetic factor which affects the shape of the uterus and the position of the fetus, or the mother's hormonal secretions influence the elasticity of all ligaments and muscles or only those of the hips.' HART (1952) dwelt briefly on CHAPPLE's theory, but it appears that no other author has suggested that maternal hormones might be of significance in the causation of congenital dislocation of the hip-joint.

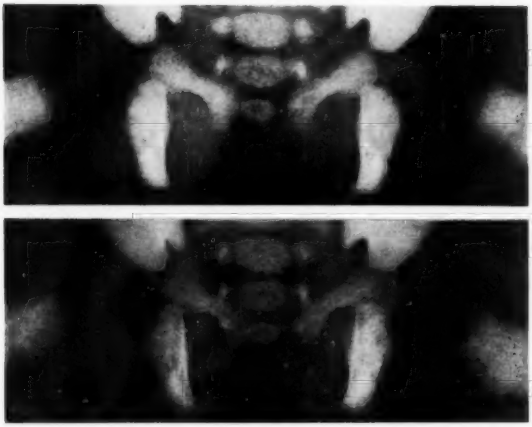

Fig. 3. *Upper*: Normal case. Legs forced posterolaterally. *Lower*: Legs forced in acetabulum. Hardly any difference in width of symphysis but increased distance between distal parts in ischia.

The fetus and the newborn have the capacity to break down certain oestrogens which cannot be resolved by adults (DICZFALUSY et coll. 1957). Girls excrete larger amounts of oestrogen in the urine than boys and for a somewhat longer period (DE BLIECK & SCHWERS 1958). In a comprehensive investigation of twins with dislocation of the hip IDELBERGER (1951) found a marked difference between enzygotic and dizygotic twins. Of 29 pairs of enzygotic twins, dislocation of the hip had occurred in both infants in 10 pairs, but in only 3 of 109 pairs of dizygotic twins. This shows that the condition can hardly be ascribed to an increased elaboration of hormone by the mother but rather to a characteristic of the child.

One might perhaps assume that the relaxation of the capsule facilitating dislocation might be produced by a decrease in the breakdown of the maternal hormones with consequent increase in their concentration and effect. The above-mentioned difference in the excretion of oestrogen with sex supports this possibility. Dislocation of the hip is also 6 times more common in girls than in boys. Hypersensitivity of the child to maternal hormones must also be considered. It has often been observed, though rarely mentioned in the literature, that women with dislocation of the hip are of a very feminine type. This extreme femininity suggests that the primary causal factor might be an increased sensitivity to oestrogen. It might also be an abnormal reaction of the connective tissue in the pelvis.

Breech presentations are about 10 times more common among children with congenital dislocation of the hip. In such cases the elongation of the

capsule may be favoured by the mechanism of delivery. Of those with congenital dislocation of the hip and delivered in the breech presentation, the ratio between females and males was only about 2: 1 as against 6: 1 for those delivered in the cephalic position. It thus appears that in some additional causal factor other than the hormonal must be involved in the breech presentation.

After the first week of life the influence of the maternal hormones has practically disappeared. Fig. 2a shows the state of the pelvis at birth and Fig. 2b, 8 days later. The instability of the symphysis pubis is now less than 1 mm, and the hips can no longer be dislocated. The only treatment the child had received was immobilization of the legs in a flexed outward position, which is the posture spontaneously assumed by newborns. But if the legs are held adducted and stretched by conventional napkins and clothing, the femoral head can, if the capsule is elongated, lie outside the acetabulum and prevent regression of the elongation with permanent partial or complete dislocation as a result. PALMÉN (1957) reported that in 14 out of 15 newborns the hip had become stable within a week and in the infants examined early in our series, the same rapid regression was observed. Dr SELANDER of the department of paediatrics of our hospital has examined more than 23 000 newborns for dislocation of the hip. He detected the condition in 36, and as far as we know not a single case had been missed. In none of the children that received immediate adequate treatment was any later dysplasia demonstrable.

It would thus appear that the aetiology of congenital dislocation of the hip-joint (which should not be confused with teratologic dislocation with multiple malformations and arthrogryposis with dislocation) may be explained. The primary factor is a marked reaction of the newborn to the maternal hormones resulting inter alia in a relaxation of the capsule of the hip-joint and symphyseal instability. It is this relaxation of the capsule that makes partial or complete dislocation of the hip possible if the legs are held in an unnatural position during the first week or so of life. The characteristic inherited is the increased reaction to the maternal hormones and not the dislocation as such. Dysplasia is a secondary phenomenon.

SUMMARY

Instability of the symphysis pubis in newborns with congenital dislocation of the hip-joint is described. It is suggested that this instability and the relaxation of the capsule responsible for the dislocation of the hip are primarily caused by maternal hormones.

ZUSAMMENFASSUNG

Es wird die Instabilität der Symphysis ossis pubis bei Neugeborenen, die an congenitaler Hüftluxation leiden, beschrieben. Es wird vermutet, dass diese Instabilität und Erschlaffung der Gelenkskapsel, die für die Dislokation der Hüfte verantwortlich ist, primär durch die mütterlichen Hormone verursacht werden.

RÉSUMÉ

L'auteur décrit l'instabilité de la symphyse pubienne chez les nouveau-nés porteurs de luxation congénitale de la hanche. Il pense que cette instabilité et le relâchement de la capsule articulaire qui est responsable de la luxation de la hanche ont comme cause première un trouble hormonal maternel.

REFERENCES

ANDRÉN, L. and VON ROSEN, S.: The diagnosis of dislocation of the hip in newborns and the primary results of immediate treatment. Acta radiol. 49 (1958), 89.

CHAPPLE, CH. C.: Congenital dislocation of the hip. *In*: NELSON, W. E.: Textbook of pediatrics, pp. 1334—1337. W. B. Saunders, Philadelphia 1954.

— and DAVIDSON, D. T.: A study of the relationship between fetal position and certain congenital deformities. J. Pediat. 18 (1941), 483.

DE BLIECK, J. et SCHWERS, J.: Influence du sexe sur la courbe d'élimination des oestrogènes chez le nouveau-né à terme. Bull. Soc. roy. belge Gynec. Obstét. 28 (1958), 476.

DICZFALUSY, E., TILLINGER, K.-G. and WESTMAN, A.: Studies on oestrogen metabolism in newborn boys. 1. Excretion of oestrone, oestradiol-17β and oestriol during the first days of life. 2. A study of the metabolism of exogeneous oestradiol-17β. Acta endocr. 26 (1957), 303.

FROELICH, M.: Traitement de la luxation congénitale de la hanche chez le nourrisson (curatif et préventif). Congrès français de chirurgie. Procès-verbaux. 24 (1911), 1048.

HART, V. L.: Congenital dysplasia of the hip joint and sequelae. Charles C. Thomas, Springfield, Ill. 1952.

HOWORTH, M. B.: Congenital dislocation of the hip. Ann. Surg. 125 (1947), 216.

IDELBERGER, K.: Die Erbpathologie der sogenannten angeborenen Hüftverrenkung. Beitr. klin. Chir. Sonderband 1951.

LANGENSKIÖLD, A. och SARPIO, O.: Patologin vid kongenital höftledsluxation belyst genom experimentell imitation av deformiteten (Swedish). Finska Läk.-Sällsk. Handl. 100 (1957), 111.

LE DAMANY, P.: La luxation congenitale de la hanche. Felix Alcan, Paris 1912.

ORTOLANI, M.: La lussazione congenita dell'anca. Capelli, Bologna 1948.

PALMÉN, K.: Dysplasia coxae congenita. (In Swedish.) Svenska Läk.-Tidn. 54 (1957), 1706.

SMITH, W. S., IRETON, R. J. and COLEMAN, C. R.: Sequelae of experimental dislocation of a weight-bearing ball and socket joint in a young growing animal. Gross alterations in bone and cartilage. J. Bone J. Surg. 40 A (1958), 1121.

GUARDIAN 125

The finest X-Ray Tube for Heavy Duty Operation

'Off Beam' Radiation factor only $\frac{1}{10}$th of level permissible by International Recommendation

The Mullard Guardian 125 is a 125kV tube specifically designed for heavy duty operation. It combines ample thermal capacity and high radiographic ratings together with Mullard Guardian protection, making it the outstanding tube for busy X-Ray departments. Ratings, specifications, etc., will be sent on request.

Mullard X-RAY DIVISION

Mullard

MULLARD LTD., X-RAY DIVISION,
NEW ROAD, MITCHAM JUNCTION,
SURREY, ENGLAND.
CABLES: MULLECTRON, LONDON.

MXR518

AECL's *new* Theratron C II

for simple, precise, economical

Now you can treat reclining or seated patients
— at intermediate or long treatment distances.

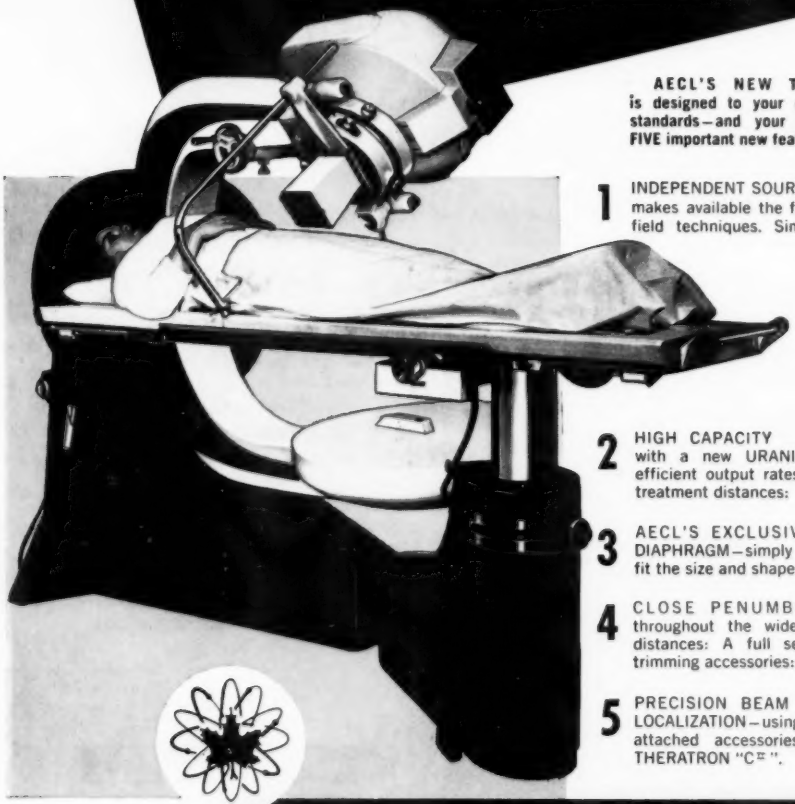

AECL'S NEW THERATRON "C II" is designed to your most exacting clinical standards—and your budget: Check these FIVE important new features:

1 INDEPENDENT SOURCEHEAD SWIVEL—makes available the full range of stationary field techniques. Simple setup procedure for upright as well as reclining patients.

2 HIGH CAPACITY — up to 50 rmm with a new URANIUM insert for highly efficient output rates at medium and long treatment distances.

3 AECL'S EXCLUSIVE EIGHT-SIDED DIAPHRAGM—simply "dial" the field to fit the size and shape of the tumour.

4 CLOSE PENUMBRA CONTROL—throughout the wide range of treatment distances. A full selection of penumbra trimming accessories.

5 PRECISION BEAM DIRECTION AND LOCALIZATION—using the range of easily attached accessories available with the THERATRON "C II".

For additional information—please write to

ATOMIC ENERGY OF CANADA LIMITED
COMMERCIAL PRODUCTS DIVISION
P.O. BOX 93 • OTTAWA • CANADA

60-2M

FROM THE RADIATION PHYSICS DEPARTMENT (DIRECTOR: ASSOC. PROF. KURT LIDÉN),
UNIVERSITY OF LUND, SWEDEN

ANGULAR AND SPECTRAL DISTRIBUTIONS OF BACKSCATTER RADIATION FROM SLABS OF WATER, BRASS, AND LEAD IRRADIATED BY PHOTONS BETWEEN 50 AND 250 keV

by

GUNNAR HETTINGER

Photons within a medium are exposed to absorption and scattering processes. It is mainly the photoelectric absorption and Compton scattering that influence photons below a few hundred keV. The coherent scattering may be neglected without introducing an error of more than a few per cent of the total absorption coefficient. After photoelectric absorption the absorbing atom may emit characteristic fluorescent radiation whose energy depends on the nuclear charge of the absorber. For heavier atoms the energy and sometimes also the intensity of the characteristic radiation are so high that the radiation must be taken into consideration in the design of shields. In a Compton process a photon collides with an electron of the absorber; this process can be repeated and on each collision the photon is degraded in energy and its direction is changed. If the process could continue uninterruptedly, it would result in photons of ever decreasing energies. The multiple scattering is about the same in all absorbers if the influence of the photoelectric absorption be neglected. However, the photoelectric absorption becomes more important at lower energies. This results in a cut-off of the energy degradation originating from multiple Compton scattering. At a certain energy, photoelectric absorption is more probable than scattering of the degraded photon, with further energy loss. This energy is

Submitted for publication 24 February 1960.

about 20 keV in water (HETTINGER and STARFELT 1959) but some hundred keV in lead (GOLDSTEIN and WILKINS 1954). Photoelectric absorption becomes important at an energy that is higher in lead than in water.

Some of the secondary photons move backwards through the surface of the irradiated medium. It is the angular and the energy distribution of this backscatter radiation that is discussed in the present paper for such scatterers as water, brass and lead. The backscatter was studied for primary photons under perpendicular incidence with energies between 50 and 250 keV.

HAYWARD and HUBBEL (1954) studied, with a scintillation spectrometer the backscatter radiation caused by primary Co^{60} radiation, and that caused by 1 MeV photons by means of Monte Carlo calculations. HINE and McCALL (1954), on the basis of an experimental investigation, described the backscattering for a point source on the scatterer as functions of geometric variables and the energy of the primary radiation; they used Hg^{203}, Cs^{137}, and Co^{60} sources. There are some other papers on Monte Carlo calculated backscatter data (PERKINS 1955 and BERGER et coll. 1955, 1956, 1960); these deal with primary photon energies above 500 keV.

LORENTZON 1954, WALSTAM 1954, and LINDELL 1954 have studied the secondary radiation from slabs of different materials. The source of primary radiation was a roentgen tube without any additional filter running at tube voltages between 70 and 160 kV. There are also some more complete investigations of secondary radiation in water for primary radiation of the therapeutic type (CORMACK et coll. 1957, and BRUCE and JOHNS 1957). However, no spectra of backscatter radiation are given in these papers. A large number of measurements on the dose build-up at the surface of a tissue-equivalent scatterer have been made (WACHSMANN et coll. 1954, JOHNS et coll. 1954 and GREENING 1954). This dose build-up, which equals the so-called backscatter factor is of the greatest importance for dosimetry in radiology.

A theoretical method for determining the approximate dose on the front face of thick slabs of iron, or elements of lower atomic numbers, has been described by CORNER and LISTON (1951). They calculated the build-up for primary gamma ray energies from 250 keV to 3 MeV with the aid of a 'modified first-order' approximation.

As yet no detailed experimental investigation appears to have been published on the differential energy and angular spectra of backscatter radiation from different materials irradiated by roentgen photons with energies below 250 keV. Such spectra are of practical importance for the calculation of radiation shields. When the scatterer consists of water, which is nearly tissue-equivalent, such spectra are of value in medical physics and radiology.

This investigation is a part of the program of our laboratory to study secondary radiation within and outside an irradiated medium. Previous papers on this subject have been published by HETTINGER and STARFELT 1959, and HETTINGER and LIDÉN 1960.

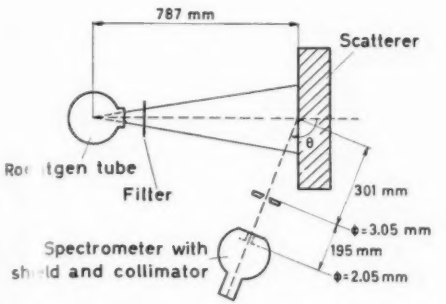

Fig. 1. Experimental arrangement for the study of radiation backscattered in the directions $\Theta = 105°$, 120°, 135°, and 157°. The NaI(Tl) scintillation spectrometer was rotated around a vertical axis through the center of the scattering surface.

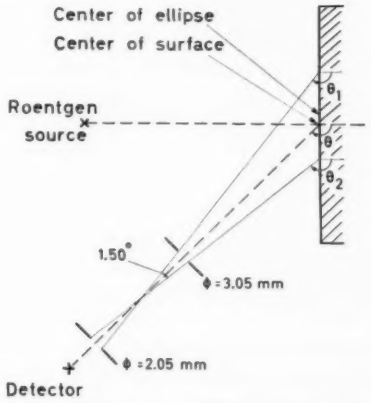

Fig. 2. Illustration of the collimating system of the detector.

Experimental

The primary radiation was produced by a roentgen generator, Müller MG 300. The output radiation was filtered by thick filters (HETTINGER and STARFELT 1958). These reduced the intensity but, on the other hand, a semimonoenergetic radiation was obtained, whose spectral shape was scarcely influenced by further absorption in, for example, 15 cm water. The dose half value layer of the primary radiation was 0.6, 2.1 and 4.5 mm Cu at tube voltages of about 100, 170, and 250 kV, respectively. The effective energies calculated from the half value layers were 63, 113, and 184 keV. The spectra of the primary radiation are drawn as dashed curves in Figs 7, 8, and 9. More detailed information about the backscatter process can be obtained for narrow bands of energy by using semimonoenergetic primary radiation. It is easy to calculate the backscatter caused by primary beams of e. g. the therapeutic type by a weighted addition of the backscatter caused by semimonoenergetic primary beams.

The experimental arrangement is shown in Fig. 1. Water, brass and lead were used as scattering media. The water phantoms were 2.5, 6.0, and 15 cm thick and the square area was 30×30 cm^2. The tanks were made of 0.4 cm thick perspex. There was a window 0.1 cm thick and 9.5 cm in diameter on the front surface, from which the backscatter radiation to be studied emerged. The brass and lead phantoms were 2.5 and 0.3 cm thick in order to correspond to semiinfinite targets.

Two circular irradiation fields were studied, 50 and 200 cm² in size. For brass and lead the field sizes corresponded to the saturation of backscatter. The center of the irradiated field coincided with the center of the front surface of the scatterer. The dose rate of the primary radiation varied about 2 per cent within the irradiated field, but at the edge of the field the dose rate was influenced by the penumbra due to the size of the focus, which was about 0.4 cm in diameter.

The focus-surface distance was 79 cm during the entire experiment. It is well known from radiology that the backscatter factor is practically independent of the focal distance. Even the so-called tumor-air ratio, which is proportional to the dose build-up in tissue, is found to be independent of the focal distance (JOHNS et coll. 1956); theoretical investigations have also confirmed this (JOHNS et coll. 1958 and BURNS 1958). The tumor-air ratio for zero depth is equivalent to the backscatter factor. This constancy of backscatter with focal distance is probably also present for scatterers other than tissue equivalent. This means that the focus-surface distance used in this experiment may be considered as infinite, i. e. the measured spectral distributions and other data in this paper correspond to a parallel primary beam under perpendicular incidence.

The NaI(Tl) scintillation spectrometer was rotated around a vertical axis through the center of the scattering surface (Fig. 1). The scintillation crystal was of the well type (HETTINGER and STARFELT 1958). Secondary radiation, corresponding to scattering angles of 105°, 120°, 135°, and 157°, was studied. The scattering angle, Θ, is measured from the central ray of the primary beam ($90° \leq \Theta \leq 180°$).

The crystal of the spectrometer 'sees' an elliptical part of the front surface of the phantom. The ellipse is defined by the intersection of this surface and the double cone generated by the two concentric collimators of the spectrometer (Figs 1 and 2). When the spectrometer is rotated to a smaller angle the ellipse becomes larger and its center moves away from the center of the irradiated field. However, the cone angle is so small (1.50°) that the latter effect can be neglected for the scattering angles studied. At 105° the half axes of the ellipse were 0.55 cm and 2.11 cm, which are much smaller than the radii of the irradiated fields (4.0 or 8.0 cm). The scatter intensity at the edge of the ellipse differs from that at the center of the phantom surface. However, the solid angle, within which the crystal is seen from the outer parts of the ellipse, is small due to the penumbra of the collimators. The scattering angle and the distance between detector and observation point vary over the ellipse (Fig. 2), but calculations have shown that these effects can be neglected.

The solid angle of the spectrometer seen from the phantom surface varies and is zero at the edge of the ellipse. This solid angle (ω) was integrated over a plane (S) through the center of the surface and perpendicular to the direction of the secondary radiation. The integral $\int \omega dS$ was found to be 6.42×10^{-4} steradian · cm².

The pulse height distributions of the backscatter radiation were measured with a multichannel analyzer of the Hutchinson-Scarrot type. The primary radiation was studied with a single channel pulse height analyzer.

Treatment of the data

The resolution of the spectrometer was 21 per cent at 63 keV, 14 per cent at 114 keV, and 11 per cent at 187 keV for monochromatic radiation. The average energy of the primary photons, $\bar{E}_P$, were 63, 114, and 187 keV. The line width of the spectrometer was thus several times smaller than the width of the spectra of primary radiation and similarly for the spectra of backscatter radiation. Consequently, no appreciable error was introduced when the correction for the limited resolution was neglected. By using a spectrometer with a crystal of the well type the escape of characteristic iodine K-radiation from the scintillator was insignificant (Fig. 14). When the spectrum of the primary radiation with $\bar{E}_P = 187$ keV was determined, it was necessary to correct for the transparency of the crystal, and for the fact that the photofraction for photons above 150 keV was less than 100 per cent. The absorption coefficients were taken from WHITE-GRODSTEIN's tables, and the photofraction data from values calculated for conventional NaI-crystals, published by MAEDER et coll. (1954).

The obtained pulse height distributions were corrected for the background, the counts lost during the dead time of the analyzer, and for the absorption in air between the source and detector and in the 0.022 cm thick aluminium window of the scintillation crystal.

The recorded spectra of backscatter radiation had to be normalized to the flux of primary photons at the observation point. In this investigation the primary and the secondary radiation were each measured in absolute units. The accuracy of these measurements depends on how well the solid angles between detector and radiation source are known. The errors are estimated to be between 5 and 10 per cent. The secondary radiation was normalized to units of photons per keV, cm^2, steradian and second, and was then correlated with the primary flux measured in units of photons per cm^2 and second at the phantom surface. Thus the angular number flux, N, was obtained in units of keV^{-1}·steradian^{-1}.

If the secondary radiation from tissue-equivalent materials is studied, the above normalization can be carried out without absolute measurements by applying the data of conventional backscatter tables (WACHSMANN et coll. 1954 and JOHNS, HUNT and FEDEROUK 1954). The backscatter factor is a measure of the relative contribution of the primary and the secondary fluxes to the dose at the surface. In several investigations dose build-up data have been used (CORMACK, GRIFFITH and JOHNS 1957; CORMACK, BURKE and DAVITT

1958; CORMACK, DAVITT, BURKE and RAWSON 1958), to match the measured secondary radiation with the primary flux.

The angular number fluxes, N, were integrated over all directions to give the integrated spectrum of backscatter radiation, N_o, (number flux) which is the total flux of secondary photons at the surface per incident primary photon

$$N_o = \int N \, d\Omega \tag{1}$$

This integral could easily be determined graphically because of the rotation symmetry at the point of interest.

Integration of the fluxes N and N_o over all energies gives build-up data. The differential angular photon number build-up, $\frac{d B_{Ph}}{d \Omega}$, was calculated from the recorded spectra according to

$$\frac{d B_{Ph}}{d \Omega} = \int N dE \tag{2}$$

and the increase, F_{Ph}, of the photon flux at the surface due to backscatter was obtained as

$$F_{Ph} = \int N_o dE \tag{3}$$

The photon number build-up was obtained when the primary or unscattered photons were added to F_{Ph}

$$B_{Ph} = 1 + \int N_o dE \tag{4}$$

The energy build-up, B_E, and the dose build-up, B_D, were calculated in a similar way. The integrands were weighted and then integrated also over the spectrum of the primary radiation.

The backscatter current characterizes the surface as a radiation source. To obtain the current, each component of the flux of the emerging radiation has to be multiplied by the cosine of the angle, φ, between the radiation direction and the normal to the surface of the scatterer. In this case, with perpendicularly incident primary photons, the angle φ equals $180° - \Theta$. The reflection power of a medium is often called albedo, A. The differential angular photon number albedo, $\frac{dA_{Ph}}{d\Omega}$, is given by the following equation

$$\frac{dA_{Ph}}{d\Omega} = \int N \cdot cos\varphi \cdot dE = cos\varphi \cdot \frac{dB_{Ph}}{d\Omega} \tag{5}$$

and the number albedo according to

$$A_{Ph} = \iint N \cdot cos\varphi \cdot dE \cdot d\Omega = \int cos\varphi \cdot \frac{dB_{Ph}}{d\Omega} \cdot d\Omega \tag{6}$$

The number albedo, A_{Ph}, is the reflected photon current and is thus always less than F_{Ph}, which is the reflected photon flux per incident photon.

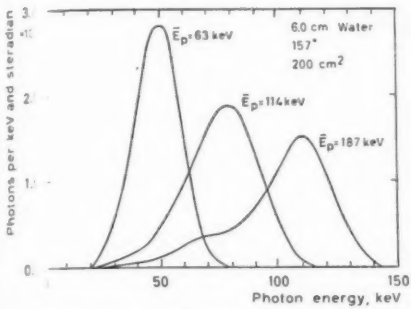

Fig. 3. Spectra of radiation backscattered in the direction $\Theta = 157°$ for the three primary qualities. Integration of the curves with respect to the photon energy yields the differential photon number build-up.

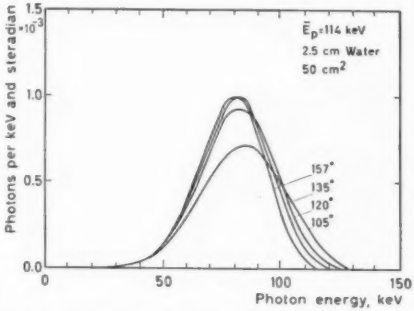

Fig. 4. Spectra of radiation backscattered in different directions ($\Theta = 105°$, 120°, 135°, and 157°) for a primary photon with $\bar{E}_P = 114$ keV. Integration of the curves with respect to the photon energy yields the differential photon number build-up.

Results and discussion

1. *Backscatter from water.* Perspex is approximately equivalent to water. The 0.1 cm perspex window of the water tanks had no influence on the recorded spectra. Measurements with a 0.5 cm thick window showed an increase of the backscatter of about three per cent.

Some spectra of scattered radiation for $\Theta = 157°$ are shown in Fig. 3. The incident primary photons had the average energies 63, 114, and 187 keV, respectively. The spectrum of backscatter radiation becomes broader with increasing primary energy. In the spectrum corresponding to $\bar{E}_P = 187$ keV there is an indication of a small peak at about 60 keV, which depends on multiply-scattered photons (HAYWARD and HUBBEL 1954, a). In the other spectra this peak is not separated. A typical change of the angular number flux with scattering angle is shown in Fig. 4. There is no marked difference in quality between backscatter radiation in different directions, not even between the once-scattered photons. The resulting energies for 114 keV photons Compton scattered once in the directions 105° and 157° are 89 and 79 keV, respectively. However, the angular spectra can depend more on the phantom thickness, as seen in Fig. 5. The peak at about 110 keV is due to mainly once-scattered photons. The number of multiply-scattered photons increases with phantom depth. An increase of the irradiated field has a similar influence.

The differential photon build-up for $\bar{E}_P = 114$ keV and 187 keV, respectively, is plotted against scattering angle in Fig. 6. The solid curves correspond to field size 50 cm² and the dashed ones to 200 cm². The values corresponding to $\bar{E}_P = 63$ keV agree within 10 per cent with those for $\bar{E}_P = 114$ keV. This is in agreement with earlier experiments (HETTINGER and LIDÉN 1960), which

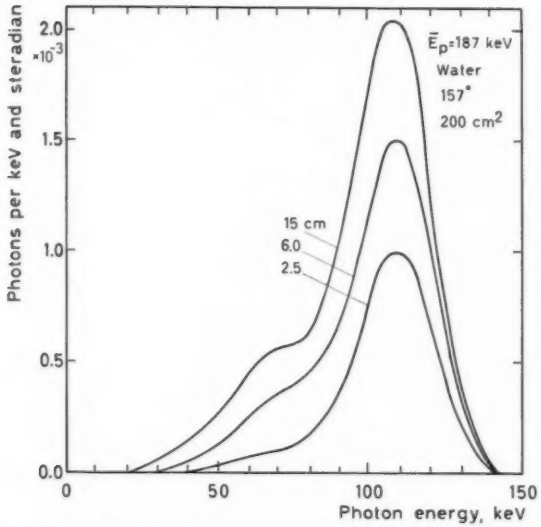

Fig. 5. Spectra of radiation backscattered in the direction $\Theta = 157°$, from water slabs of different thicknesses. Integration of the curves with respect to the photon energy yields the differential photon number build-up.

showed that the photon build-up within a water phantom was almost independent of the primary photon energy when this was between 50 and 250 keV. Curves corresponding to the same field size seem to meet at $\Theta = 90°$, and curves corresponding to the same phantom thickness meet at $\Theta = 180°$. This means that saturation of scattered photons in the direction $\Theta = 90°$ is obtained for a phantom thickness of less than 2.5 cm. In this direction the intensity of the scattered radiation is influenced most by the field size. For scattering angles of about 180° the secondary radiation is more dependent on the phantom depth. For other angles the differential number build-up is a complicated function of both field size and phantom depth.

The angular number fluxes were integrated over space according to eq. (1). The resulting spectra are shown in Figs 7, 8, and 9. The dashed curves correspond to one primary photon, and the solid curves to the corresponding number flux of radiation backscattered from water phantoms of different thicknesses of 2.5, 6.0, and 15 cm. It is clear that most of the backscatter flux is built up in the first 5 cm of the scatterer (Fig. 10). The quality of the backscatter radiation does not vary appreciably when the phantom thickness is increased from 2.5 to 15 cm (Table 1), nor when the field size is varied. Table 2 shows the average energy of the photons of the flux backscattered from a 15

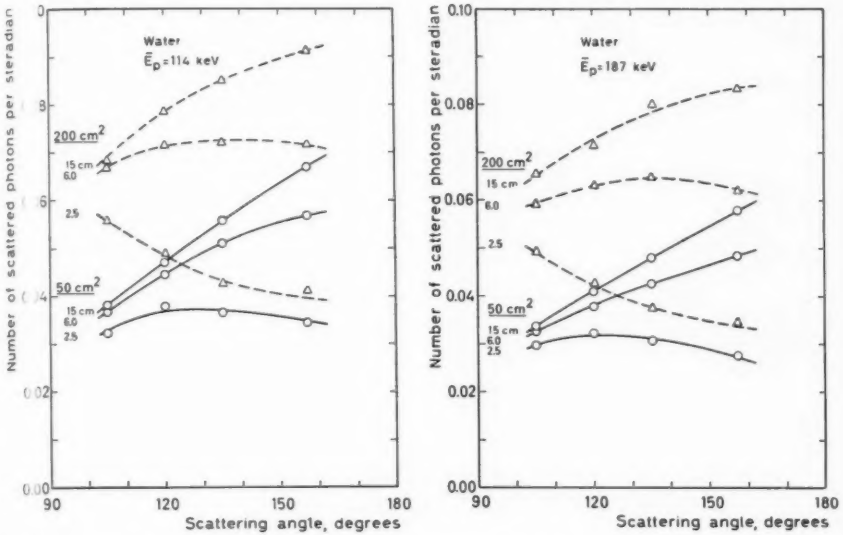

Fig. 6. Differential photon number build-up at the center of the irradiated field per incident primary photon, with $\bar{E}_P = 114$ keV, or $\bar{E}_P = 187$ keV, respectively.

Table 1

Characteristics of backscatter flux. Average energy of secondary photons, $\bar{E}_S$, in comparison with average energy of primary photons, $\bar{E}_P$, calculated for different thicknesses, d, of the water phantom. Field size: 50 cm².

$\bar{E}_P$ (keV)	$\bar{E}_S$ (keV) for different thicknesses		
	2.5 cm	6.0 cm	15 cm
63	51	51	50
114	81	80	77
187	113	109	107

Table 2

Characteristics of backscatter flux. Average energy of secondary photons, $\bar{E}_S$, in comparison with average energy of primary photons $\bar{E}_P$, calculated for different field sizes. Water phantom: 15 cm thick.

$\bar{E}_P$ (keV)	$\bar{E}_S$ (keV) for different field sizes	
	50 cm²	200 cm²
63	50	50
114	77	75
187	107	105

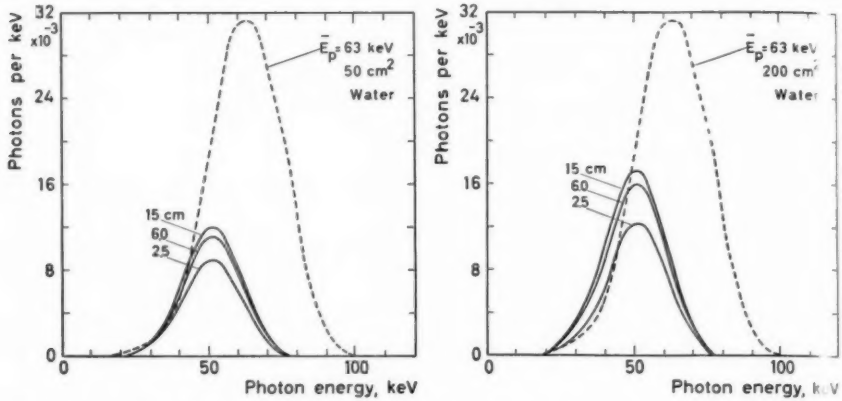

Fig. 7. Number flux of radiation backscattered (solid curve) at the phantom surface corresponding to one incident primary photon with $\bar{E}_P = 63$ keV (dashed curve). Integration of both curves together yields the photon number build-up at the center of the irradiated field.

Table 3

Photon number build-up at the center of front surface of water phantom

$\bar{E}_P$ (keV)	Phantom thickness (cm)	B_{Ph} for field sizes 50 cm²	200 cm²
	2.5	1.22	1.31
63	6.0	1.29	1.41
	15	1.30	1.44
	2.5	1.22	1.31
114	6.0	1.28	1.43
	15	1.30	1.48
	2.5	1.19	1.27
187	6.0	1.23	1.38
	15	1.25	1.45

cm thick phantom irradiated with different field sizes. The average energy is between 60 and 80 per cent of the average primary photon energy. The energy degradation is of course greatest for the primary photons of highest energy.

The photon number build-up is given in Table 3. As mentioned previously the values corresponding to different primary photons are roughly equal. The table shows that the F_{Ph} value, eq. (3), is about 0.5 in the center of a 200 cm² field on a 15 cm thick phantom. This means that the backscatter flux is about 50 per cent of the primary flux when the numbers of photons are counted. How-

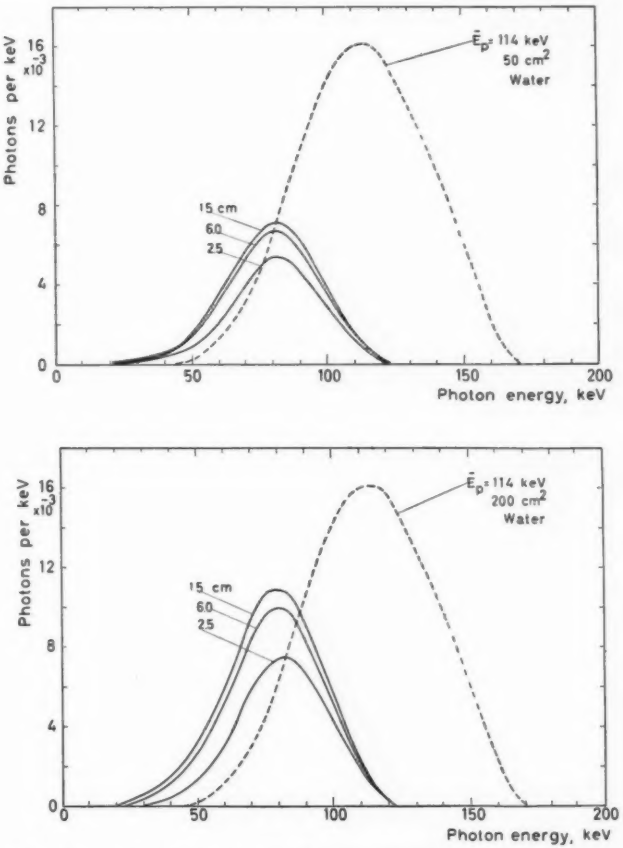

Fig. 8. Number flux of radiation backscattered (solid curve) at the phantom surface corresponding to one incident primary photon with $\bar{E}_P$ = 114 keV (dashed curve). Integration of both curves together yields the photon number build-up at the center of the irradiated field.

Table 4

Energy build-up at the center of front surface of a 15 cm thick water phantom

$\bar{E}_P$ (keV)	B_E for field sizes	
	50 cm²	200 cm²
63	1.27	1.35
114	1.20	1.32
187	1.15	1.25

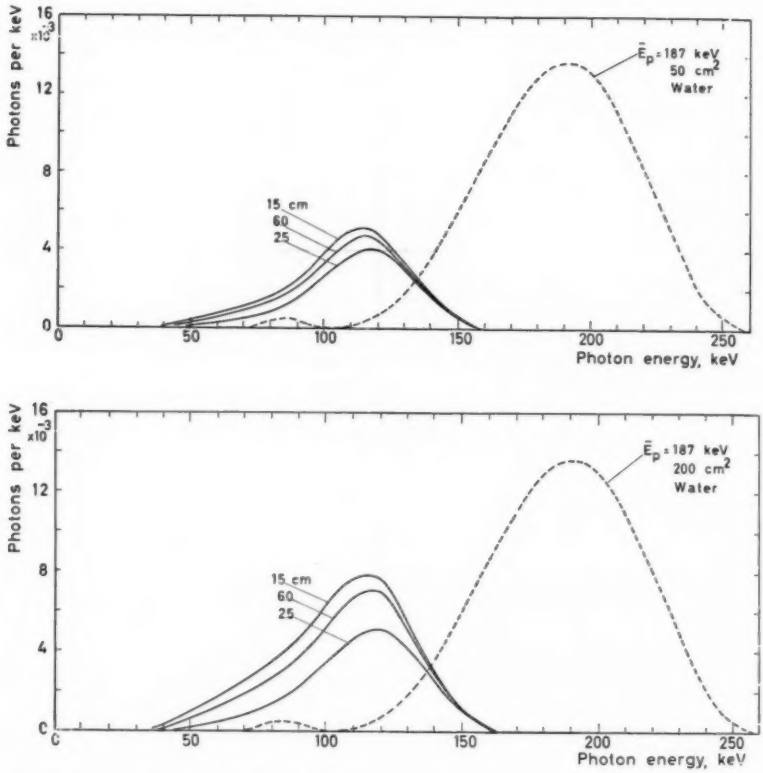

Fig. 9. Number flux of radiation backscattered (solid curve) at the phantom surface corresponding to one incident primary photon with $\bar{E}_P = 187$ keV (dashed curve). Integration of both curves together yields the photon number build-up at the center of the irradiated field.

ever, the corresponding number albedo is about 0.25, which signifies that the number of secondary photons emerging from a small area round the center of the phantom surface is about 25 per cent of the number of primary photons incident upon the same area. Some of the build-up values are plotted against phantom thickness in Fig. 10. The solid curves correspond to $\bar{E}_P = 114$ keV and the dashed ones to $\bar{E}_P = 187$ keV. The curves corresponding to 200 cm² may indicate that saturation is not reached with a phantom 15 cm thick. However, the error introduced in the backscatter number flux is small if saturation in phantom depth is assumed to be present for both field sizes studied. Dose

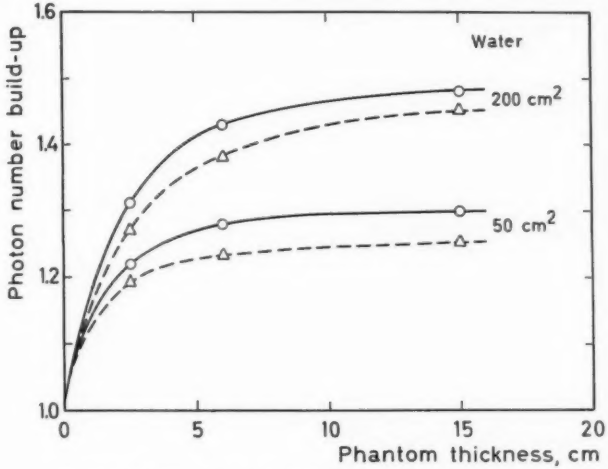

Fig. 10. Photon number build-up at the center of the irradiated field plotted against phantom thickness. The solid curves correspond to $\bar{E}_P = 114$ keV and the dashed ones to $\bar{E}_P = 187$ keV.

measurements by WACHSMANN et coll. support this assumption. The energy and dose build-up values are presented in Tables 4 and 5. These values vary with phantom thickness in a manner similar to the photon build-up, Fig. 10.

Water is nearly tissue-equivalent, and dose backscatter factors for primary beams of the radiologic type were calculated and compared with tabulated data. The method of calculation has been described by HETTINGER and LIDÉN (1960). The comparison is shown in Table 6 and values necessary for the

Table 5

Dose build-up at the center of front surface of a water phantom

$\bar{E}_P$ (keV)	Phantom thickness (cm)	B_D for field sizes 50 cm²	200 cm²
	2.5	1.25	1.35
63	6.0	1.32	1.47
	15	1.34	1.51
	2.5	1.16	1.23
114	6.0	1.21	1.32
	15	1.22	1.35
	2.5	1.10	1.15
187	6.0	1.12	1.20
	15	1.13	1.23

Table 6

Dose backscatter factors for two kinds of primary radiation used in radiotherapy calculated from present experiment compared with tabulated data

Reference	B_D			
	170 kV + 0.5 mm Cu, HVL = 1.0 mm Cu Field size		250 kV + 1.5 mm Cu, HVL = 2.4 mm Cu Field size	
	50 cm²	200 cm²	50 cm²	200 cm²
Johns et coll. (1954)	1.29	1.42	1.21	1.33
Deduced from present experiment	1.28	1.43	1.20	1.33

Table 7

Percentual composition of two kinds of primary radiation used in radiotherapy and values necessary for calculation of the dose backscatter factors given in table 6

$\bar{E}_P$ (keV)	Dose from one average primary photon per cm² (r)	Percentual composition of primary radiation used in radiotherapy	
		170 kV + 0.5 mm Cu HVL = 1.0 mm Cu	250 kV + 1.5 mm Cu HVL = 2.4 mm Cu
63	$3.64 \cdot 10^{-11}$	60	26
114	5.2	40	49
187	9.5	0	25

calculation are given in Table 7. The good agreement between the experimental and tabulated data indicates that the measured spectral distributions, both primary and secondary, are correct in magnitude and in shape.

It is easy to calculate the once-scattered radiation with the aid of known absorption and scattering cross-sections. The energy of once-scattered photons can be calculated from the energy of the unscattered photons with the aid of the Compton equation.

Several papers are available (Payne-Scott 1937, Lindell 1954, Johns et coll. 1958, Cormack and Johns 1958, and others) in which the quantity and quality of first-order scatter radiation are calculated. The calculation for the present geometric conditions with the point of interest at the center of the irradiated field on the phantom, is illustrated in Fig. 11. The parallel primary beam is perpendicularly incident upon the medium and the number of photons scattered through one Compton process in the direction Θ is to be calculated.

The primary flux at the depth x in the medium is

$$P \cdot e^{\mu - P x} \qquad \text{(photons per cm}^2\text{)} \qquad (7)$$

where P is the primary flux before the scatterer and μ_P is the attenuation coeffi-

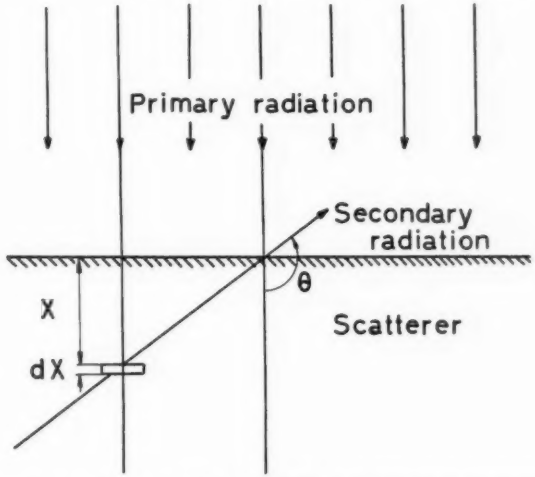

Fig. 11. Illustration for the calculation of first-order radiation backscattered in the direction Θ. The parallel primary beam is perpendicularly incident upon the scatterer.

cient. The current in the direction Θ of photons scattered once from an infinitesimally thin disk at the depth x is given by

$$\left(\frac{d\sigma}{d\Omega}\right)_{\Theta} \cdot P \cdot e^{-\mu_P x} \cdot dx \qquad \text{(photons per cm}^2\text{ and steradian)} \qquad (8)$$

where $\left(\frac{d\sigma}{d\Omega}\right)_{\Theta}$ is the Klein-Nishina cross-section. Consequently the flux in the same direction is

$$-\left(\frac{d\sigma}{d\Omega}\right)_{\Theta} \cdot \frac{1}{\cos\Theta} \cdot P \cdot e^{-\mu_P x} \cdot dx \quad \text{(photons per cm}^2\text{ and steradian)} \qquad (9)$$

On the way to the surface these scattered photons are attenuated by a factor

$$e^{\mu_S \cdot \frac{x}{\cos\Theta}} \qquad (90° \leq \Theta \leq 180°) \qquad (10)$$

where μ_S means the attenuation coefficient of the secondary radiation in question. Geometrical considerations show that the first-order scatter flux at the surface is given by

$$-P \cdot \left(\frac{d\sigma}{d\Omega}\right)_{\Theta} \cdot \frac{1}{\cos\Theta} \int_0^{\infty} e^{-x\left(\mu_P - \frac{\mu_S}{\cos\Theta}\right)} \cdot dx \qquad (11)$$

The effective thickness, l, of the irradiated part of the scatterer is influenced by both the field size, radius r, and the phantom thickness, d. It is determined according to

$$\begin{cases} l = d, & d \leq -r \cdot \cot \Theta \\ l = -r \cdot \cot \Theta, & -r \cdot \cot \Theta \leq d \end{cases} \tag{12}$$

Consequently the differential photon number build-up caused by once-scattered photons, $\left(\frac{dB_{Ph}}{d\Omega}\right)_1$, is given by

$$\left(\frac{dB_{Ph}}{d\Omega}\right)_1 = \left(\frac{d\sigma}{d\Omega}\right)_\Theta \cdot \frac{1}{\mu_S - \mu_P \cdot \cos \Theta} \cdot G \tag{13}$$

where G is a geometric factor. It is dimensionless and depends on the saturation condition in the scatterer according to

$$G = 1 - \epsilon^{-l\left(\mu_P - \frac{\mu_S}{\cos \Theta}\right)} \tag{14}$$

If the primary beam is inhomogeneous, eq. (13) has to be integrated over the spectrum of the primary radiation. In the present investigation, with semi-monoenergetic primary radiation, this integration could be excluded when the single scattering was calculated.

When the geometric factor G equals unity, the differential first-order build-up, corresponding to saturation condition, is obtained from eq. (13) (Table 8). The differential Compton scattering cross-sections necessary for the calculation were taken from NELMS's graphs. The values in Table 8 are about 0.04 steradian^{-1} in all directions for the primary photons studied. The attenuation coefficients μ_P and μ_S result mainly from Compton scattering and only to a lesser extent from photoelectric absorption. This explains why the two first factors in eq. (13) together are relatively constant, while each factor shows a greater gradient.

The geometric factor G is always positive and smaller than or equal to unity, and it indicates the part of the maximal first-order backscatter that is developed. Table 9 shows the G factor for 114 keV primary photons. The values at $\Theta = 105°$

Table 8

Differential first-order build-up at front surface of a semi-infinite water medium

$\bar{E}_P$ (keV)	$\left(\frac{dB_{Ph}}{d\Omega}\right)_{\Theta, 1, \text{saturation}}$ (steradian^{-1})			
	$\Theta = 105°$	120°	135°	157°
63	0.041	0.038	0.039	0.041
114	0.042	0.038	0.038	0.039
187	0.039	0.035	0.034	0.033

Table 9

Geo tric factor, G, for 114 keV primary photons. The factor indicates that part of the maximal first-orde backscatter (Table 8) developed at the center of a given field size on a water phantom of given thickness.

ield size	Phantom thickness			G	
(cm²)	(cm)	$\Theta = 105°$	120°	135°	157°
	2.5	0.71	0.70	0.65	0.59
50	6.0	0.71	0.70	0.81	0.89
	15	0.71	0.70	0.81	0.97
	2.5	0.88	0.73	0.65	0.59
200	6.0	0.92	0.91	0.92	0.89
	15	0.92	0.91	0.97	1.00

are nearly the same for the different depths. In this scattering direction the field size matters more than the phantom thickness. However, the opposite condition is indicated by the table for the largest scattering angle studied (157°). The same behaviour was observed for the experimentally determined differential photon number build-up in Fig. 6. Table 10 shows the quotient between the theoretically calculated first-order scatter and the experimentally determined total backscatter in different directions for $\bar{E}_P = 114$ keV. The value corresponding to the other two primary qualities differ from those given in Table 10 by less than 10 per cent. The multiple scattering increases relatively with increasing field, phantom size and scattering angle.

The composition of the number fluxes is given in Table 11. At the integration over all directions the differential build-up receives the weight *sin* Θ, which is greatest at $\Theta = 90°$. The values in Table 11 therefore correspond to the composition of the backscatter in the direction Θ somewhere between 105° and 120°. Roughly half of the backscatter flux consists of once-scattered radiation for the geometric configurations and primary qualities which are often used in radiotherapy.

Table 10

Percentual contribution of the first-order scatter to the differential photon number build-up. The water phantom was irradiated by primary photons with $\bar{E}_P = 114$ keV.

Field size	Phantom thickness	$\left(\frac{dB_{Ph}}{d\Omega}\right)_{\Theta\text{-}1} \Big/ \left(\frac{dB_{Ph}}{d\Omega}\right)_{\Theta}$ (%)			
(cm²)	(cm)	$\Theta = 105°$	120°	135°	157°
	2.5	92	70	67	67
50	6.0	81	60	60	60
	15	78	57	55	56
	2.5	66	57	58	55
200	6.0	57	48	48	48
	15	56	44	43	42

Table 11

Percentual contribution of first-order scatter photons to the backscattered flux. The water phantom was irradiated by primary photons with $\bar{E}_P = 114$ keV.

Field size (cm^2)	Phantom thickness (cm)	$F_{Ph,\,1}/F_{Ph}$ (%)
50	2.5	79
	6.0	69
	15	67
200	2.5	61
	6.0	52
	15	49

2. *Backscatter from brass.* Brass is approximately equivalent to copper. The lead content was negligible. The phantom was about 5 mean free paths thick for the primary radiation studied and could be regarded as a semi-infinite medium (BERGER and DOGGET 1956). An irradiated area of 200 cm^2 gave a maximal build-up in the center of the field. The cross section of photoelectric absorption is greater in brass than in water. It is thus to be expected that the backscatter from brass is less intense.

The differential photon number build-up calculated from experiment is shown as the solid line in Fig. 12. It is nearly constant for all scattering angles. In the Monte Carlo calculations of albedos of aluminium by PERKINS the differential photon number build-up of backscatter originating from perpendicularly incident Co^{60} radiation proved also to be nearly constant in all directions.

The number flux of backscatter radiation integrated over space is shown in Fig. 13. The radiation scattered from brass is somewhat harder than that from water. The low energy end of the spectrum is at about 40 keV. The multiple scattering process is cut off at this energy due to photoelectric absorption. The average energy of the integrated backscatter flux and the corresponding photon and energy build-up are shown in Table 12. It indicates that the F_{Ph} value of brass is one sixth and one third of that of water for the primary qualities $\bar{E}_P$ = 114 keV and 187 keV, respectively.

The contribution of single scatter is indicated by the dashed lines in Fig. 12. An integration over space shows that 75 per cent and 66 per cent of the back-

Table 12

Characteristics of backscatter radiation from a semi-infinite brass medium

$\bar{E}_P$ (keV)	$\bar{E}_S$ (keV)	B_{Ph}	$F_{Ph,\,1}/F_{Ph}$ (%)	B_E	A_{Ph}
114	89	1.08	75	1.07	0.04
187	121	1.17	66	1.10	0.08

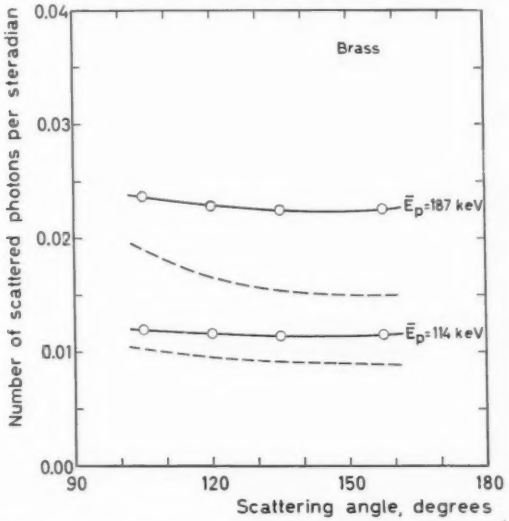

Fig. 12. Differential photon number build-up (solid lines) per primary photon incident upon the surface of a semi-infinite brass medium. Dashed lines correspond to calculated first-order scatter.

scatter photon flux is made up of singly-scattered photons for $\bar{E}_P = 114$ keV and 187 keV, respectively (Table 12). Thus only the smaller part of the backscatter consists of multiply-scattered photons, because of the great photoelectric absorption. However, at higher primary energies the multiple scattering becomes more developed. Monte Carlo calculations of the reflected roentgen rays, resulting from perpendicularly incident Co^{60} radiation on aluminium, show that about three quarters of the backscatter consist of photons scattered more than once (PERKINS).

Table 12 also gives data on the number albedo. It is about half of the corresponding F_{Ph} value. The number albedos agree with those determined by BERGER and RASO (1960) with Monte Carlo calculations.

The characteristic fluorescent radiation at 8 keV and lower energies produced by photoelectric absorption in brass is negligible. Its intensity can be calculated from an equation similar to eq. (13). The G factor is put equal to one, and the differential cross section which is constant in all directions is given by

$$\left(\frac{d\sigma}{d\Omega}\right)_{\Theta} = \frac{1}{4\pi} \cdot \delta_K \cdot \omega_K \cdot \tau_P \qquad (15)$$

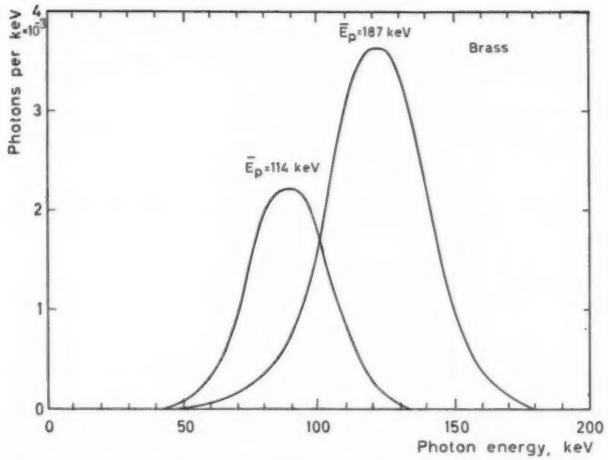

Fig. 13. Number flux of the radiation backscattered from a semi-infinite brass medium irradiated by perpendicularly incident primary photons with $\bar{E}_P = 114$ keV or $\bar{E}_P = 187$ keV, respectively.

where τ_P is the photoelectric absorption coefficient of the primary photons, δ_K indicates the fraction of photoelectric processes taking place in the K-shell (about 80 per cent) and ω_K is the K-fluorescence yield (BURHOP). In eq. (13) μ_S was replaced by μ_K, the absorption coefficient for the characteristic K-roentgen rays. In this case of brass, $\mu_P \cdot cos\ \Theta$ could be neglected in comparison with μ_K. Calculations showed that the number of K-photons was two or three orders of magnitude smaller than the number of backscatter photons due to Compton processes.

3. *Backscatter from lead.* The radiation backscattered from a semi-infinite lead medium consisted mainly of characteristic K-fluorescent radiation at about 75 keV. A resulting pulse height distribution is shown in Fig. 14. Calculations showed that about two per cent of the pulses came from photons scattered through one Compton process. However, these pulses could not be separated. The small peak at about 45 keV is due to the so-called iodine K-escape pulses. The main peak at 75 keV is somewhat slanted and broadened owing to the different K-lines whose energies and relative intensities are illustrated by the arrows in Fig. 14.

The angular photon number build-up is shown in Fig. 15. The solid lines are from experiment, while the dashed ones are calculated according to eqs (13) and (15), which give the K-roentgen photons originating from unscattered primary photons. Eq. (13) was integrated only over the part of the spectrum

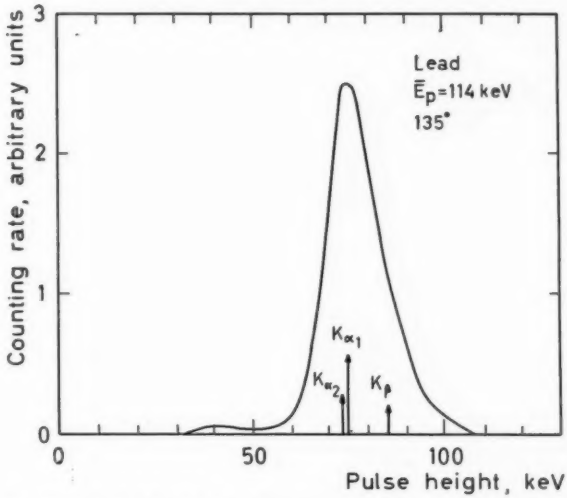

Fig. 14. Pulse height distribution corresponding to the radiation backscattered from a semi-infinite lead medium. Most of the pulses are due to characteristic *K*-fluorescent radiation. The arrows indicate the energy and relative intensity of different lead *K*-lines. The small peak at about 45 keV is due to so-called iodine *K*-escape pulses.

of the primary radiation that was above the *K*-absorption edge at 88 keV, because photons of lower energy cannot give rise to characteristic lead *K*-radiation. The discrepancies between the experimental and theoretical curves in Fig. 15 can partly depend on small errors in the energy calibration of the spectrum of the primary radiation and on errors in the absorption coefficients.

The contribution from lead *L*-radiation can be neglected. In this experiment the energy of the primary radiation was too high to give characteristic *L*-radiation with an intensity high enough to be comparable with the characteristic *K*-radiation and the Compton scattered radiation together. It was found that primary photons with energies somewhat above an absorption edge give rise mainly to corresponding characteristic radiation whereas the contribution of Compton scattered radiation is prominent only for primary photons with energies far above the *K*-absorption edge. Compton scattered radiation contributes only about half of the reflected radiation from a semi-infinite lead target irradiated by Co^{60} radiation (HAYWARD and HUBBEL, see Handb. Phys.).

The values of B_{Ph}, B_E and A_{Ph} calculated from the experimental data are presented in Table 13. The number albedo of lead for $\bar{E}_p = 114$ keV is about three times that of brass. Nearly 10 per cent of the incident energy is reflected as lead *K*-radiation. However, at $\bar{E}_p = 187$ keV the reflectivity of lead is equal to or somewhat lower than that of brass.

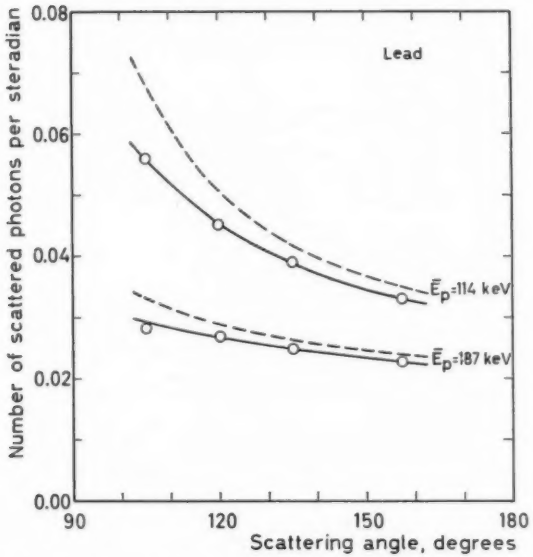

Fig. 15. Differential photon number build-up (solid lines) due to characteristic lead K-radiation per primary photon incident upon the surface of a semi-infinite lead medium. Dashed lines correspond to calculated values.

The angular distributions of the backscatter radiation from semi-infinite slabs of brass and lead were systematically different. For brass the differential photon number build-up was nearly constant in all directions (Fig. 12), but for lead the differential build-up originating from characteristic fluorescent radiation had its maximum at $\Theta = 90°$ (Fig. 15). For primary photon energies high enough to make $\mu_P \ll \mu_K$, the differential build-up becomes constant in all directions but, at the same time, also smaller according to eqs (13) and (15).

Table 13

Characteristics of backscatter radiation from a semi-infinite lead medium

$\bar{E}_P$ (keV)	$\bar{E}_S$ (keV)	B_{Ph}	B_E	A_{Ph}
114	75	1.29	1.19	0.12
187	75	1.17	1.07	0.08

Acknowledgements

The investigation was supported by grants from the Swedish Cancer Society. The author wishes to express his thanks also to Assoc. Prof. K. Lidén for invaluable advice and criticism.

SUMMARY

The energy distribution of radiation backscattered in different directions was measured in absolute units with a NaI-scintillation spectrometer. The recorded spectra were integrated over space to give the backscatter number flux. Build-up and albedo were calculated. Good agreement with backscatter factors was obtained. Once-scattered radiation and characteristic fluorescent radiation were theoretically calculated. The backscatter from brass and lead consisted mainly of, respectively, once-scattered radiation and characteristic K-radiation.

ZUSAMMENFASSUNG

Die spektrale Verteilung der Rückstrahlung in verschiedenen Richtungen wurde mit einem NaJ-Scintillationsspektrometer in absoluten Einheiten gemessen. Die erhaltenen Spektra wurden über alle Richtungen integriert, um den Photonenfluss der Rückstrahlung zu erhalten. 'Build-up' und albedo wurden kalkuliert. Gute Übereinstimmung mit Rückstreufaktoren wurde erhalten. Einmal-gestreute Strahlung und charakteristische Fluoreszenzstrahlung wurden theoretisch berechnet. Die Rückstrahlung von Messing und Blei bestand hauptsächlich aus einmal-gestreuter Strahlung bzw. charakteristischer K-Strahlung.

RÉSUMÉ

La distribution d'énergie du rayonnement diffusé en retour dans différentes directions a été mesurée en unités absolues au moyen d'un spectromètre à scintillation à cristal de NaI. Les spectres enregistrés ont été intégrés dans l'espace pour mesurer le flux diffusé en retour. La répartition d'énergie et l'albedo ont été calculées. On a obtenu une bonne concordance avec les facteurs de diffusion en retour. Le rayonnement ayant subi une seule diffusion en retour et le rayonnement de fluorescence caractéristique ont été calculés théoriquement. Le rayonnement diffusé en retour par le laiton et par le plomb consistent principalement, respectivement en rayonnement diffusé une seule fois et en radiation K caractéristique.

REFERENCES

BERGER, M. J.: Reflection and transmission of gamma radiation by barriers: Monte Carlo calculation by a collision density method. J. Res. Nat. Bur. Stand. 55 (1955), 343.

— and DOGGET, J.: Reflection and transmission of gamma radiation by barriers: Semianalytic Monte Carlo calculation. J. Res. Nat. Bur. Stand. 56 (1956), 89.

— and RASO, D.: Monte Carlo calculations of gamma ray backscattering. Radiat. Research 12 (1960), 20.

BRUCE, W. R. and JOHNS, H. E.: Monte Carlo calculations on the spectrum of scattered radiation produced in water by X-ray beams of interest in radiotherapy. Radiology 68 (1957), 100.

BURHOP, E. H. S.: The Auger effect and other radiationless transitions. Cambridge University Press, Cambridge 1952.

BURNS, J. E.: Letter to the editor. Brit. J. Radiol. 31 (1958), 643.

CORMACK, D. V. and JOHNS, H. E.: Spectral distribution of scattered radiation from a kilocurie Cobalt 60 unit. Brit. J. Radiol. 31 (1958), 497.

— Burke, D. G. and Davitt, W. E.: Spectral distributions of 140 kVp X-rays. Radiology 70 (1958), 91.
— Griffith, T. J. and Johns, H. E.: Measurement of the spectral distribution of scattered 400 kVp X-rays in a water phantom. Brit. J. Radiol. 30 (1957), 129.
— Davitt, W. E., Burke, D. G. and Rawson, E. G.: Spectral distributions of 280 kVp X-rays. Brit. J. Radiol. 31 (1958), 565.
Corner, J. and Liston, R. H. A.: Back-scattering of gamma-rays from a thick slab. Proc. Roy. Soc. 204 (1951), 323.
Goldstein, H. and Wilkins Jr, J. E.: Calculations of the penetration of gamma rays. United States AEC, Report NYO-3075 (1954).
Greening, J. R.: A survey of surface back-scatter factors for radiation generated at 200 to 250 kV. Brit. J. Radiol. 27 (1954), 532.
Handbuch der Physik. Band XXXVIII/2, S. 810. Springer Verlag, Berlin, Göttingen und Heidelberg 1959.
Hayward, E. and Hubbel, J. H.: The backscattering of the Co^{60} gamma rays from infinite media. J. Appl. Phys. 25 (1954, a), 506.
— — The albedo of various materials for 1-MeV photons. Phys. Rev. 93 (1954, b), 955.
Hettinger, G. and Lidén, K.: Scattered radiation in a water phantom irradiated by roentgen photons between 50 and 250 keV. Acta radiol. 53 (1960), 73.
— and Starfelt, N.: Bremsstrahlung spectra from roentgen tubes. Acta radiol. 50 (1958), 381.
— — Improved NaI scintillation spectrometer for the study of continuous X-ray spectra. Nucl. Instr. 3 (1958), 25.
— — Energy and angular distribution of scattered radiation in a water tank irradiated by X-rays. Ark. Fysik 14 (1959), 497.
Hine, G. J. and McCall, R. C.: Gamma-ray backscattering. Nucleonics 12: 4 (1954), 27.
Johns, H. E., Bruce, W. R. and Reid, W. B.: The dependence of depth dose on focal skin distance. Brit. J. Radiol. 31 (1958), 254.
— Hunt, J. W. and Federouk, S. O.: Surface back-scatter in the 100 kV to 400 kV range. Brit. J. Radiol. 27 (1954), 443.
— Morrison, M. T. and Whitmore, G. F.: Dosage calculation for rotation therapy. Amer. J. Roentgenol. 75 (1956), 1105.
Lindell, B.: Secondary roentgen radiation. Acta radiol. 41 (1954), 353.
Lorentzon, L.: Secondary roentgen radiation from wax, Al, Fe, and Pb at tube voltages between 40 and 170 kV. Acta radiol. 41 (1954), 201.
Maeder, D., Müller, R. und Wintersteiger, V.: Über die Linienform monochromatischer gamma-Strahlung in Szintillationsspektrographen. Helv. Phys. Acta 27 (1954), 3.
Nelms, A. T.: Graphs of the Compton energy-angle relationship and the Klein-Nishina formula from 10 keV to 500 MeV. Nat. Bur. Stand. Circular No. 542 (1953).
Payne-Scott, R.: The wave length distribution of the scattered radiation in a medium traversed by a beam of X or gamma rays. Brit. J. Radiol. 10 (1937), 850.
Perkins, J. F.: Monte Carlo calculation of gamma-ray albedos of concrete and aluminium. J. Appl. Phys. 26 (1955), 655.
Wachsmann, F., Heckel, K. und Shirren, C. G.: Die Grösse der Rückstreuung bei verschiedener Tiefe des Streukörpers. Strahlenther. 94 (1954), 161.
Walstam, R.: Dose measurements on secondary roentgen radiation. Acta radiol. 41 (1954), 348.
White Grodstein, G.: X-ray attenuation coefficients from 10 keV to 100 MeV. Nat. Bur. Stand. Circular No. 583 (1957).

FROM THE RADIOTHERAPY DEPARTMENT (CHIEF PHYSICIST: L. H. S. CLARK),
LAMBETH HOSPITAL, LONDON, ENGLAND

A CALCULATOR FOR DETERMINING ACTIVITIES OF SPECIMENS FROM THEIR OBSERVED COUNT-RATES

by

W. E. LIVERSAGE

When radioactive specimens are measured on a counting system of known sensitivity, mathematical corrections have to be made for the background and the dead time of the counting system so as to convert the observed count-rates into true ones. These must then be divided by the sensitivity factor, applicable to the particular isotope being measured, to determine the activities of the specimens. The calculator described below performs the above mathematical operations, thus enabling the observed count-rates to be converted directly into microcuries.

Description of the instrument. The calculator consists of a base board on which is mounted a sheet of 3-cycle log-log graph paper. Attached to the left hand side of the board is a brass rod parallel to the O-Y axis of the graph paper (see the schematic figure). Mounted on, and at right angles to the rod, is a perspex rule which may be moved up or down the rod in the direction of the O-Y axis. When the clamping knob F is unscrewed, the rule may be moved sideways in a direction at right angles to O-Y but is constrained by guides always to remain parallel with the O-X axis. On the underside of the perspex rule is inscribed a line, also parallel with the O-X axis, and which is graduated with a 4-cycle logarithmic scale identical to that of the graph paper and numbered 0.01 to 100 μc.

Submitted for publication 6 February 1960.

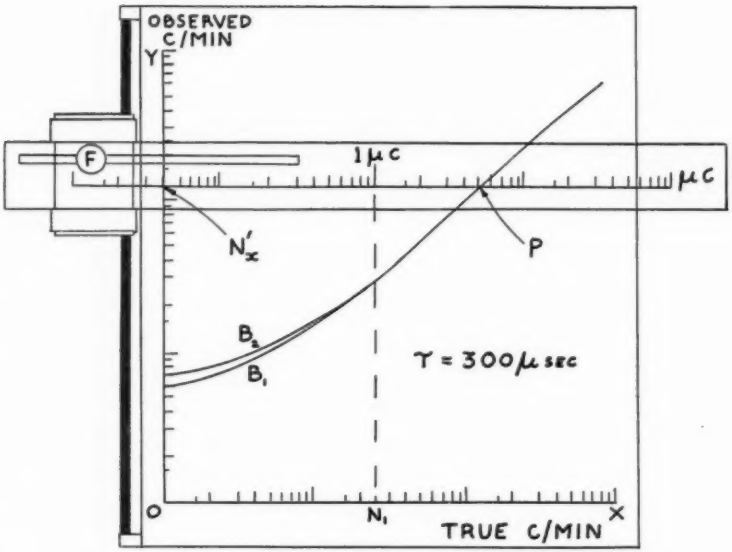

Schematic illustration of the instrument.

With any counting system, the true counts/min N is related to the observed counts/min N' by the following equation

$$N = \frac{N'}{1 - N'\tau} - B$$

where τ is the dead time of the counting system in minutes and B is the background counts/min. Using this formula, a curve is drawn on the graph paper, plotting observed counts/min along the O-Y axis against true counts/min along the O-X axis for a given value of background. A series of such curves may be drawn to cover the range of values of background likely to be obtained in practice for values of true count-rate varying from 100 to 100 000 counts/min. These curves converge at high count-rates.

Method of application

Suppose a specimen gives N'_x observed counts/min when the background is B_1 counts/min and the sensitivity of the counting system is N_1 true counts/min/μc. Then, to find the activity of the specimen the following procedure may be used:

. Move the perspex rule sideways so that 1 μc on the rule lies on the vertical th ough N_1 true counts/min on the O-X axis, and screw down the clamping kn b F.

I. Move the perspex rule up the rod until the inscribed line coincides with N observed counts/min. The point P on the rule where the curve B_1 cuts the μc scale is then the activity of the specimen at the time of measurement.

hould the activity of the specimen be required at some subsequent time t, wh n its activity will have decayed to say d %, then the activity of the specimen at his subsequent time may be found by setting the $\frac{d}{100}$ μc graduation instead of he 1 μc graduation on the vertical through N_1. The activities of specimens at ome preceding time may similarly be found by setting the $\frac{100}{d}$ μc graduation on the vertical through N_1.

Should measurements be made on a series of similar specimens on the same apparatus, operation (I) above need only be carried out once as this operation simply sets the rule so that it applies to the sensitivity of the counting system being used.

Theory. The activity A_x of any specimen at the time of measurement is determined by the relationship

$$A_x = \frac{N_x}{N_1}$$

where N_x is the true counts/min with the specimen, and N_1 is the true counts/min with 1 μc of the same isotope.

$$\therefore \text{Log } A_x = \log N_x - \log N_1 \qquad (1)$$

Now suppose the distance of any graduation numbered N counts/min on the graph is $k \log \frac{N}{100}$ to the right of point O, where k is a constant depending on the graph paper available. Then, when operations (I) and (II) above have been carried out, the abscissa of point P will be N_x true counts/min and will be a distance to the right of the 1 μc graduation equal to

$$k \log \frac{N_x}{100} - k \log \frac{N_1}{100} = k \, (\log N_x - \log N_1)$$

But, by equation (1) this distance will be $k \log A_x$.

Thus, if the horizontal perspex rule is graduated with a log scale such that the distance of any graduation numbered A μc is a distance $k \log A$ to the right

of the 1 μc graduation (*i. e.* if the log scale on the perspex rule has the same constant k as the graph paper) then point P will coincide with the graduation on the rule equal to the activity of the specimen at the time of measurement.

The activity A'_x at some subsequent time t is given by the relationship

$$A'_x = \frac{N_x}{N_1} \times \frac{d}{100} \qquad 2)$$

and if now $\frac{d}{100}$ μc on the perspex rule is set on the vertical through N_1 true counts/min on the graph, point P will be a distance to the right of the 1 μc graduation equal to

$$k\ (\log N_x - \log N_1 + \log \frac{d}{100})$$

(This is actually a smaller distance than before as $\log \frac{d}{100}$ will be negative.)

But, from (2) above

$$\log N_x - \log N_1 + \log \frac{d}{100} = \log A'_x$$

Thus point P will now coincide with graduation A'_x which is the activity of the specimen at the required time t.

Acknowledgements

I wish to thank Dr. L. H. S. Clark for his kind advice and encouragement in this work. I am also indebted to Mr. W. J. Chantrill who made the instrument.

SUMMARY

A simple calculator is described which performs the mathematical operations necessary to convert directly into microcuries the observed count-rates in a radioactive specimen.

ZUSAMMENFASSUNG

Ein einfacher Rechner, der die Umrechnung der in einem radioaktivem Präparat registrierten Strahlungsenergie direkt in Mikrocurie duchführt, wird beschrieben.

RÉSUMÉ

L'auteur décrit une machine calculatrice simple qui effectue les opérations mathématiques nécessaires pour convertir directement en microcuries les taux de comptage enregistrés sur une préparation radio-active.

BOOK REVIEWS

X-RAY DIAGNOSIS OF THE ALIMENTARY TRACT IN INFANTS AND CHILDREN. By Edward B. Singelton. 352 pages, 215 illustrations. Year Book Publishers, Chicago 1958. Price: 11 dollars.

Radiodiagnosis began to be applied in the paediatric field almost as soon as the science of diagnostic radiology in general came into existence, in other words over 60 years ago. It has, however, only become more widely accepted as a 'specialty within a specialty' during the past few decades. This is largely due to developments in paediatric surgery, which have now made it possible successfully to treat many diseases that previously were only accessible to symptomatic treatment. With expanding surgical success, there has arisen a need for more exact diagnostic methods, and this has been an important incentive to the use of roentgenographic techniques in children. Singelton's book, which comprises 350 pages, contains a comprehensive bibliography as well as an index. The illustrations are numerous, but as is often the case with American publications, the quality of the reproductions leaves much to be desired. The elementary examination technique is described in detail, but in the reviewer's opinion this is unnecessary. As radiologists working with paediatric radiodiagnosis must first have a thorough mastery of roentgenographic techniques in general, it would have been better to describe only such modifications of these as are necessary to meet the special conditions prevailing in children and their diseases. The sections on developmental and paediatric anatomy, physiology and pathology, which contain exactly the right amount of information for the radiologist, are especially valuable. Singelton emphasizes the value of fluoroscopy as a complement to the roentgen films, but he does not mention the possibility, and desirability, of reducing the fluoroscopic dose in children through the use of an image intensifier. The examination of the abdomen is systematically based on conventional films (scout-film examination) taken with a horizontal beam, and demonstrates clearly that such examinations alone often give sufficient information to serve as a guidance for the treatment of the child. Examinations by means of a barium meal are often of less value, and may even be dangerous as they may delay an operation. A contrast enema, on the other hand, is often indispensable. The author has disposed and concentrated his subjects well; the book is easy to read and gives clear evidence not only of an extensive knowledge of the literature but also of wide personal experience. Although the reviewer is not entirely in agreement with Singelton on all points, the book can be recommended and forms a valuable complement to a work such as Astley's 'Radiology of the Alimentary Tract in Infancy'.

H. Gladnikoff

LA FLEBOGRAFIA VERTEBRALE TRANSOMATICA. By G. Marcozzi, S. Messinetti, L. Sara a, and M. Colombati. 159 pages, 80 illustrations, 20 tracings, and bibliography. Ediz ni Mediche e Scientifische, Roma 1959. Price: 6 500 lire.

This monograph describes an original method of phlebography of the vertebral nd azygo-caval systems. The vertebral body is punctured percutaneously and the cont st medium injected into the spongiosa. By due consideration of the haemodynamic fac rs it is possible to achieve selective filling of the different parts of the deep thoraco-abdom al veins.

A review of developments in the roentgen examination of the vertebral and azygo-caval systems is first presented, particular attention being devoted to intraosseous phlebography. Next follows an anatomy treatise based mainly on the work of BATSON. It is stated that the corticalis on the lateral aspect of the vertebral body is thin and easily perforated by means of special needles; the spongiosa is described as a 'sponge of blood'. The puncture is aimed at the venous network in the horizontal middle plane of the vertebral body, which drains directly into the extra- and intravertebral plexuses. These plexuses have wide communications with the azygo-caval system, mostly through avalvular veins. Among the factors influencing the direction of the blood stream and the flow of the contrast medium which are considered are: the site of puncture, the positioning of the patient and the tilt of the table, as well as the intrathoracic pressure, which can be modified by control of the breathing under general anaesthesia.

The technique was developed in an experimental investigation in dogs under normal conditions as well as after ligation at different levels of the venae cavae or of the arch of the azygos vein. This study allowed important conclusions to be drawn regarding the adaptation of the method for use in human subjects: the puncture, under roentgen control, is easy and safe; anatomical and histologic studies of sacrificed animals fail to show any changes due to infection, necrosis or trauma; puncture of the thoracic vertebrae, which involves certain risks, may be avoided; by taking the above-mentioned haemodynamic factors into consideration it is possible, by puncture of the lumbar or cervical vertebrae, to demonstrate any part of the respective vertebral, azygos, and inferior and superior caval systems.

The examination in human subjects was performed under general anaesthesia, and so far only normal cases have been investigated. The contrast medium was injected in an amount of 50 ml within 10 seconds and roentgenograms in two projections were obtained during and shortly after the injection. No side effects were observed.

The illustrations are all of excellent quality, and tracings help to explain the roentgenograms. The method of intravertebral injection, to judge by this material, seems to offer interesting possibilities and to enable good results to be obtained.

The book does not escape criticism, however. The method of percutaneous catheterization of the femoral veins for the examination of the iliac veins and of the inferior vena cava, is only just mentioned; it is discarded in a few words in the foreword as one involving excessive loss of blood. It is also surprising to find that the authors seem to ignore several important publications recording results obtained with the same method; at any rate they are not included in the bibliography. An assessment of the value of the authors' technique in comparison with other procedures is therefore not possible.

J. Roulleau

CRÂNE ET FACE DANS LA MALADIE DE PAGET. Par J. A. Lièvre et H. Fischgold. 132 pages, 75 illustrations. Masson, Paris 1959. Price: 40 NF.

This monograph represents the close cooperation of a rheumatologist and a radiologist and shows that the methods of roentgen examination of the skull and face in osteitis deformans (Paget's disease) warrant detailed consideration.

The material presented consists of 75 cases, which were selected from a series of 389 patients examined during the ten-year period 1947—1957. All types and stages of Paget's disease in various parts of the skull and face have been included. The follow-up examinations in some cases extend up to 11 years and cover the early stages as well as the progress of the disease. Many will find the book useful as a guide in the choice of a suitable roentgen technique (including tomography, direct fine-focus enlargement and logetronic improvement of the roentgenograms). The chapters dealing with osteoporosis circumscripta and the characteristic roentgenologic changes in the calvarium and the petrous bone with special reference to the differential diagnosis are of particular value. Malignant degeneration and carcinomatous metastases appearing in Paget's disease of the skull are illustrated. The roentgen findings in relation to the clinical signs as well as the relationship between osteitis deformans and other conditions are discussed and the various pathologic and pathogenetic problems are considered.

The style of the book is clear and concise and the wide experience of the authors is reflected in the text; a general survey of the literature is included. The illustrations are of excellent quality and well chosen and are provided with full legends. The volume is poorly bound but is beautifully printed.

J. Roulleau

KLINIK UND PRAXIS DER UROLOGIE. Band I und II. Von W. Staehler. 1 755 Seiten, 1 675 Abbildungen. Georg Thieme, Stuttgart 1959. Price: DM 480.

This massive work consists of a comprehensive and systematic survey of urology. The author in the preface emphasizes 'die innige Verflechtung von Urologie and Roentgenologie' and the book is profusely illustrated with roentgenograms. Many of these — and almost always the retrograde pyelograms — are of poor quality and not acceptable in a handbook; furthermore, the legends do not always correspond to what is evident in the alternate negative and positive reproductions. The other illustrations are often excellent.

The description of such a simple procedure as the demonstration of whether calcifications lie within or outside the kidney (Figs. 185—187, for example) seems to disclose a lack of sense of elementary techniques and the sections on angiography suggest that the author is not entirely familiar with the literature and modus operandi. It is only to be regretted that roentgen diagnostics with their wide variety of methods, so important in urology, should be dealt with in such an amateurish fashion in an obviously important book. Elaborate reproductions of roentgenograms involve heavy expenditure, and in their own interests, as well in those of purchasers, the publishers should have engaged some competent person to examine the films and ensure that they were suitable for reproduction.

Olle Olsson

RÖNTGENDIAGNOSTIK BEIM NEUGEBORENEN UND SÄUGLING. Von Hermann G. W f. 317 Seiten, 370 Abbildungen. Wilhelm Maudrich Verlag, Wien-Bonn-Bern 19 9. Price: 90 DM.

This work is divided into three parts covering the skeletal system, the thorax, nd the abdominal organs, respectively. The skeletal system is only summarily treated as this subject is being dealt with in a separate publication from the same clinic with S o-boda as author.

The text is concise and gives in a concentrated form the essential clinical and ro nt-genographic aspects of the majority of current diseases which are encountered at th se ages. A number of rare, or comparatively unusual, conditions are also described nd illustrated. Space has been saved by refraining from including any literature refere ces in the text at the expense of the profuse illustrative material. Extensive bibliograp ies at the end of each main section comprise a good selection of the pertinent American nd European literature in the respective fields. They together amount to no less than 1 500 items. In a work of this kind it is naturally always a matter of opinion as to what should be included and what omitted. The reviewer would certainly consider the urological section as being treated too summarily. Thus, for example, the value of micturition urethrocystography is only briefly commented upon, and no illustrations are included. This seems regrettable in view of the fact that adequate surgical treatment depends largely on such an examination. The author's opinion that micturition roentgenograms can only with difficulty be obtained in infants is not shared by the reviewer. The differential diagnosis between a Wilm's tumour and a neuroblastoma does not appear to be clarified by the statement that the localization is decisive. Heart diagnostics are, as in most general surveys in the field of pediatric roentgenology, treated somewhat cursorily. The inclusion of some characteristic illustrations of a vascular ring would have been well justified. As mentioned in the text, definite roentgenographic criteria of thymus hyperplasia and thymus enlargement in the range of ages dealt with do not seem to exist, but more emphasis could have been placed on this fact since the terms are nevertheless used in the legends. This observation is important because unjustified over-confidence in diagnoses of this nature have often led to misdirected therapeutic measures. The differential diagnosis of anterior pleuritis mediastinalis should no longer be a problem.

These comments are not meant to reflect upon the essential value of this work. The excellent illustrative material deserves the highest praise, and the book can be warmly recommended to roentgenologists as well as to pediatricians.

Ulf Rudhe